Study on kinetic behavior during ohmic heating pasteurization and quality evaluation of liquid eggs: experimental and computer simulation analysis

Master's Thesis

Study on kinetic behavior during ohmic heating pasteurization and quality evaluation of liquid eggs: Experimental and computer simulation analysis

September 2021

Graduate School of Marine Science and Technology
Tokyo University of Marine Science and Technology
Master's Course of Food Science and Technology

Wang Chunsen

Master's Thesis

Study on kinetic behavior during ohmic heating pasteurization and quality evaluation of liquid eggs: Experimental and computer simulation analysis

September 2021

Graduate School of Marine Science and Technology
Tokyo University of Marine Science and Technology
Master's Course of Food Science and Technology

Wang Chunsen

[修士]

修士学位論文内容要旨
Abstract

専　攻 Major	Food Science and Technology	氏　名 Name	Wang Chunsen
論文題目 Title	Study on kinetic behavior during ohmic heating pasteurization and quality evaluation of liquid eggs: Experimental and computer simulation analysis		

【Background and Objective】

Food manufacturers prefer liquid egg products instead of eggs in shell because they have advantages such as lower microbiological risk and less storage space requirement. Ohmic heating (OH) can avoid disadvantages such as, nutrition loss, sensory changes, and energy losses compared with conventional. However, Although OH is considered as a volumetric uniform heating method, some non-uniformities in temperature distribution could occur with a direct impact into accomplish pasteurization standards in delicate samples such as liquid eggs. In this study, an OH system (20 kHz, 50 V) was applied for the pasteurization of liquid eggs (whites, yolks, and whole eggs). The aims were to predict the kinetic behavior of the liquid eggs using numerical calculation by the finite element method (*FEM*) and to obtain the appropriate heating conditions to achieve the pasteurization standards for each sample while retaining the quality attributes experimentally and by computer simulation.

【Materials and Methods】

OH experiment: Liquid eggs were heated by an OH machine (FJB-5.5; Frontier Engineering Co. Ltd., Japan) at 20 kHz and 50 V from 20℃ to the target temperature (59.1℃ for whites and wholes, and 63.3℃ for yolks) to avoid unnecessary thermal protein denaturation. Then the OH was stopped and the liquid egg samples were kept inside the thermal insulation chamber to continue the pasteurization using the residual temperature. The sample temperatures at center and top-corner during processing were measured by fiber-optic sensors.

Pasteurization effect and quality evaluation: Pasteurization standards (*P*-value) of *Salmonella typhimurium* and thermal protein non-denaturation ratio (*X*) were calculated and modeled using developed 3D models and kinetics models, respectively. From both the hot and cold spots of the samples, the temperature, *X*, and pasteurization profiles were estimated. Color changes were also evaluated using a computer vision system.

Model establishment for simulation: COMSOL Multiphysics 5.6 was used for the simulations of ohmic pasteurization of liquid eggs in this study. Two different 3-D models were developed in this study and applied to four simulation approaches (two like the experimental experiment and two considering the use of an external heating system) to visualize the temperature and distribution of degrees of pasteurization at several cross sections.

【Results and Discussion】

Although liquid egg samples achieved the target temperature in a short time, hot and cold spots during OH process were identified by 3D simulation at the center and surface regions, respectively. It can be due to the contact between sample and chamber and the slight heat losses of samples to the air along the tangential direction near the electrodes. The heating conditions were optimized according to a high constant *X* value, a low total color difference value ($\Delta E < 3$), and certain pasteurization standards for each sample. No significant differences were found for the color values of each sample before and after OH plus thermal keep approach (10 min) while high *X* values were obtained (0.87, 0.89, and 0.96 for whites, whole eggs,

and yolks, respectively). It was found that OH combined with a concurrent external heating approach was successful in reducing non-uniformities in temperature, which could accomplish the *P*-value standards for liquid egg samples while avoiding excessive thermal protein denaturation caused by local overheating. Using this approach, liquid egg white, whole egg, and egg yolk could achieve the pasteurization standard after 422, 1083, and 603 s, respectively, while keeping *X* values at 0.88, 0.69, and 0.93, respectively. OH synergistically used with external heating methods are of potential value for the design of ohmic pasteurization systems for liquid eggs.

Contents

Chapter 1 – Introduction

1.1 Background and objective

1.1.1 Background

Hen egg is a rich and well-balanced source of essential nutrients for human diet composed by proteins (around 6.25 g per egg), fatty acids (around 4.33 g per egg), various trace minerals (around 94.2 mg per egg), and vitamins (around 0.77 mg per egg) (ORKA, 2021), of high biological value (Stadelman et al., 1995). In fact, egg protein is of such high quality that it is used as the standard by which other proteins are compared. Eggs have a biological value (efficacy with which protein is used for growth) of 93.7%. Comparable values are 84.5% for milk, 76% for fish, and 74.3% for beef (ORKA, 2021).

With the development of the breeding industry and the increase in market demand, the worldwide production of hen eggs in shells has been steadily increasing in recent decades, achieving more than 83.48 million tons in 2019 (FAO, 2021). Unfortunately, outbreaks of diseases caused by *Salmonella* in raw eggs continue to pose a public health threat (CDC, 2018; EFSA & ECDC, 2011). To avoid this problem, food manufacturers prefer liquid egg products (whole eggs, yolks, and albumen) instead of eggs in the shell because they are easier to handle, have a lower microbiological risk, have a longer shelf life, and require less storage space (Li et al., 2005; Nemeth et al., 2011).

Conventional pasteurization methods based on thermal transfer have disadvantages such as the temperature non-uniformity during processing, which makes it hard to achieve the pasteurization standard while avoiding the quality change due to local overheating, and the energy efficiency of the conventional surface heating methods were only 10–15%, reported by Lagunas-Solar et al., (2005). As a novel pasteurization method, ohmic heating (OH) can avoid some problems such as overheating, loss of nutritional value, sensory changes, and energy losses observed when conventional thermal processing methods (e.g., HTST pasteurization and UHT sterilization) are used (Cappato et al., 2017; Nakai et al., 2018). Products processed via OH tend to have a better quality, including structural integrity, flavor, and nutrient retention, compared with those processed using conventional heating (Seyhun et al., 2013). Unfortunately, non-uniform temperature distribution during OH has also been reported (Cappato et al., 2017). The temperature distribution and the location of “cold spots” during the OH process need to be considered especially since its effects cannot be extrapolated from the current knowledge of conventional heating (Knirsch et al., 2010). Therefore, the assessment of uniform temperature distributions during OH processes is particularly important. Marra, et al. (2009) pointed out that when applying OH on food

products, mathematical models of the progressing, as an invaluable aid for understanding and validation of thermal technologies, should be developed to identify possible hot and cold spots, in order to quantify heat losses and to evaluate the influence caused by main factors on the product during the thermal progress, thus ensure completely safe of products treated by OH. Guo, et al. (2017) conducted OH for four types of two-component foods with non-uniform electrical conductivity (EC) at high frequencies and established mathematical model as well as computational work. The results of experiments and simulations showed good agreements, which proved the practicability of applying OH associated with mathematical methods.

From the changes of physicochemical properties and quality attributes of egg products (such as, color (Koç et al., 2011; Llave et al., 2018a), viscosity (Sánchez-Gimeno et al., 2006), emulsifying properties (Monfort et al., 2012a), and foaming and gelling properties (Alamprese et al., 2019) due to the application of thermal process, color is one of the most studied attributes because egg color affects the acceptability of many egg-based products. Most of these changes have been related to the non-homogeneous degree of thermal protein denaturation, which varies depending on the target component in the egg. However, to the best of our knowledge, the relationship between the degree of pasteurization and the thermal protein denaturation of liquid eggs has not been studied in detail for OH applications at high frequencies, to assure not only quality retention but also food safety.

1.1.2 Objective

In this study, liquid egg samples (egg whites, yolks, and whole eggs) were OH-treated at 20 kHz from room temperature to the target temperature with the aim of effectively pasteurizing the sample and to attempt high-quality attribute retention, focusing on thermal protein denaturation and color changes. Four pasteurization approaches, including OH and an external heating system, were evaluated via 3-D computer simulation models by the finite element method (FEM) using COMSOL Multiphysics 5.6. The specific aims of this study were to:

1. using OH method at high frequency (20 kHz) to heat liquid egg white, yolk, and whole egg for pasteurization;
2. measuring temperature profiles and electrical properties of samples and calculating EC values during OH, then investigating the relationship between temperature and electrical conductivities of the materials at high frequency (20 kHz).
3. identify the hot and cold spots of liquid egg samples during processing by analyzing the temperature

distribution via computer simulation;

4. evaluate the pasteurization effect (*P*-value) against *Salmonella typhimurium* and the thermal protein non-denaturation ratio (*X*) of liquid egg samples during OH processing by numerical simulation;
5. analyze the color change of liquid egg samples after OH processing via computer vision system (CVS); and
6. optimize the heating conditions to ensure that the liquid egg samples achieved the required degree of pasteurization while retaining quality attributes (especially color and thermal protein denaturation).

1.2 Literature review

1.2.1 Traditional pasteurization methods

In food industry, the conventional thermal processing (HTST pasteurization and UHT sterilization) is still the main technique to ensure microbiological safety of processed foods (Goullieux & Pain, 2005). However, it has certain disadvantages such as, overheating, sensory changes, nutrition loss, and low energy efficiency because of the heat transfer mechanisms (conduction and convection) involved (Sakr & Liu, 2014).

1.2.2 Novel pasteurization methods for liquid eggs

Novel pasteurization methods for eggs have been explored in recent years, such as non-thermal treatment technologies including pulsed electric fields, high hydrostatic pressure, ultraviolet light, ultrasound waves, and ozone processing, since liquid eggs are very sensitive to high heating temperatures (Amiali et al., 2007; de Souza & Fernández, 2011; Huang et al., 2006; Monfort et al., 2012b; Perry et al., 2011). However, these non-thermal treatment approaches have been reported to have some limitations in inactivating certain pathogens (Monfort et al., 2012c). Microwave (MW) and ohmic heating (OH) have also gained attention in recent years. The MW process can rapidly heat eggs in the shell, but some problems have been observed, such as the non-uniform heating of egg whites and yolks, and the difficulty of maintaining the desired temperature after stopping the MW process (Dev et al., 2008). More details of OH were shown in the following section.

1.2.3 Ohmic heating for food processing

Ohmic heating (OH) is defined as a process wherein electric current is passed through materials with the

primary purpose of heating them via the conversion of electrical into thermal energy, resulting generally in a rapid and uniform temperature increase within the food (Cappato et al., 2017). OH applied to foods is known since 19th century (De Alwis & Fryer, 1990), being first applied to milk pasteurization, and have been studies by many scientists over the years, and many improvements were made. Nowadays, OH has been applied to blanching, evaporation, dehydration, fermentation, extraction, thawing foods, sterilization, and pasteurization (Cappato et al., 2017).

The principal mechanism of microbial inactivation during the OH process is thermal in nature, and it has an additional non-thermal effect at low frequencies (usually 50-60 Hz) (Knirsch et al., 2010). On the other hand, OH at these low frequencies shows an increase in electromechanical reactions and erosion of the electrodes (Jaeger et al., 2016). This factor is relevant because direct contact between the food and electrodes is believed to be a key aspect of the application (Guo et al., 2017). These are some of the reasons for the recent increase in OH applications at high frequencies (≥ 10 kHz). The advantages of the application of OH at high frequencies instead of low frequencies have been reported in the literature. Examples of this include reducing the incidence of fouling during milk processing (Bansal & Chen, 2006), minimizing the texture degradation of peach flesh (Shynkaryk et al., 2010), and increasing the electrical conductivity (EC) of yellowtail (S*eriola quinqueradiata*) fillets and beef blocks (Jin et al., 2015 and Llave et al., 2018b, respectively).

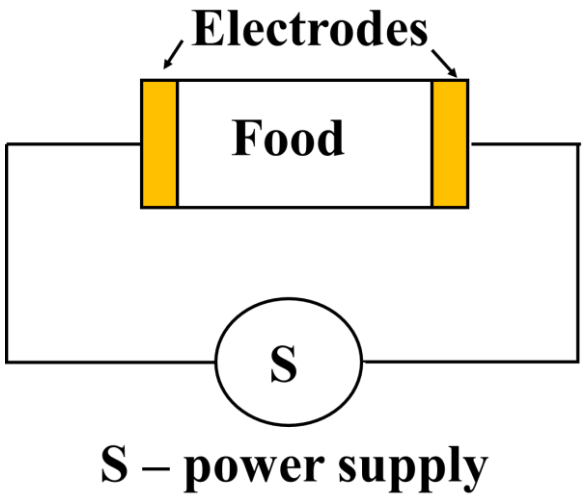

Fig. 1-2 Schematic diagram of working principle circuit of OH

1.2.4 Pasteurization effect of liquid eggs

The pasteurization effect was evaluated by the pasteurization value (*P*-value), which is defined as the effect achieved through equivalent time (in minutes) of heating at required pasteurization temperature (Horn et al., 1997). The current Food Safety and Inspection Service (FSIS) regulations of USA governing the processing of egg products require the use of a combination of times and temperatures for pasteurization in order to inactivate Salmonella in liquid eggs (CFR, 2020). For example, the pasteurization requirement for liquid whole eggs (60 ℃ for 3.5 min) is expected to achieve a relative 8.75-log reduction of *Salmonella* (ARS, 1969). The requirements for liquid egg white and yolk are 56.7 ℃ for 3.5 min and 61.1 ℃ for 3.5 min, respectively (CFR, 2020).

And the pasteurization standard in this study referenced to the thermal pasteurization requirement for liquid eggs of MHLW (1959): 54℃ × 10 min，58℃ × 10 min, and 59℃ × 10 min for liquid egg white, whole egg, and egg yolk, respectively.

1.2.5 Finite element method

Finite element method (*FEM*) is a numerical method which contribute to solve the matters appearing in mathematical physis and engineering. Mainly, it is an effective method for solving matters related with heat transfer, mass transport, structure analysis, electromagnetic field. One of the important advantages of it is finding approximate solutions to boundary value problems for partial differential equations, converting the complex structure or equations into simper parts aimed to calculate relatively easy as well.

FEM is widely used in modeling analysis. for example, Wu and Taylor (2003) combined the finite element method (*FEM*) with boundary element method (*BEM*) to clarify the nonlinear interaction relation between water waves and bodies. Baaijens et al. (2004) tried to use mixed *FEM* to do the viscoelastic fluid flow analysis with goal of obtaining precision, efficient computation methods. In addition, the results suggested that this method also can be applied to computation for the method can't be as closed-form differential methods. Stefanou (2009) illustrated the potential direction in further of *FME* used for computer simulation.

1.3 Structure of this dissertation

This dissertation consists of five parts, and contents of each part are briefly stated as below.

In chapter 1, the backgrounding including the current status (huge production of raw shell egg products,

the problems such as *Salmonella* infection, et al.) of egg industry, the potential of liquid egg products was introduced and the objective of this research was explained. Literatures about the pasteurization methods for liquid eggs development; the history, mechanism, and advantages of ohmic heating were reviewed, and the potential of this technology in food industry was proved, which both provided basic theory for our research.

The outline of this dissertation was also presented in chapter 1.

In chapter 2, the electrical conductivity (EC) of liquid eggs (including egg whites, egg yolks, and whole eggs) during OH were measured, which was one of the most important factors in OH study. The liquid egg samples were heated by a OH machine under 50 V and 20 kHz from room temperature (20 ℃) to target temperature (59.1 ℃ for egg white and whole egg, 63.3 ℃ for egg yolk) to avoid unnecessary thermal protein denaturation. An amperemeter and a voltmeter (Digital Multimeter DT4282; HIOKI, Japan) were connected to the OH system to measure the current and voltage to calculate the EC of liquid egg samples during the OH process.

In chapter 3, temperature history during ohmic heating approach (stopped when the temperature of liquid eggs achieved target temperature to avoid unnecessary thermal protein denaturation) and thermal keep approach (to continue thermal pasteurization with residual thermal) of liquid egg samples at two different locations (center and top-corner) were measured by fiber-optic sensors. Pasteurization standards (*P*-value) of *Salmonella typhimurium* and thermal protein non-denaturation ratio (*X*) were calculated depending on the temperature profiles of samples during processing (including approaches 1 and 2). From both the center and top-corner (assumed hot and cold spots) of the samples, the temperature, *X*, and pasteurization profiles were estimated. Color changes were also evaluated using a computer vision system.

In chapter 4, numerical simulation via finite element method (*FEM*) was done using software COMSOL Multiphysics 5.6 in this study. Two different 3-D models were developed in this study and applied to four simulation approaches to obtain the simulated results of temperature profiles , *P*-values, and *X* values of liquid egg samples:

(1) Model 1 (to verify the experimental results)

Approach 1: OH process only, as shown in experimental approach 1 in Chapter 3.

Approach 2: OH process and thermal keep approach, as experimental approach 2 in Chapter 3.

(2) Model 2 (to optimize the heating conditions to accomplish the pasteurization standards for liquid egg samples while avoiding excessive thermal protein denaturation caused by local overheating by computer simulation).

Approach 3: OH process plus an external heating approach, which started after the OH process ended. The liquid egg samples were heated via OH (50 V, 20 kHz) from 20 °C to T_t (step 1), which was then changed into an external heating system (heating temperature kept at T_t, step 2).

Approach 4: OH plus concurrent external heating approach. The liquid egg samples were heated via OH (50 V, 20 kHz) and the concurrent external heating system (temperature of it was set 1 °C higher than the center temperature of the egg sample) from 20 °C to T_t (step 1). After reaching T_t, OH was stopped, and the external heating temperature was set to maintain the T_t (step 2).

In chapter 5, results and conclusions from chapters above were summed up. Ohmic heating synergistically used with external heating methods of liquid egg samples was evaluated and the method to obtain the temperature distribution including hot and cold spots of food samples via computer simulation was discussed. The progress and defects of the technology were mentioned, in order to provide references for the modification and optimization in real operations. The potential of ohmic heating technology for delicate samples such as liquid egg products was thought to be possible.

1.4 References

Alamprese, C., Cigarini, M., & Brutti, A. (2019). Effects of ohmic heating on technological properties of whole egg. *Innovative Food Science and Emerging Technologies*, 58, 102244.

Amiali, M., Ngadi, M. O., Smith, J. P., & Raghavan, G. S. V. (2007). Synergistic effect of temperature and pulsed electric field on inactivation of *Escherichia coli O157: H7* and *Salmonella enteritidis* in liquid egg yolk. *Journal of Food Engineering,* 79(2), 689–694.

Bansal, B., & Chen, X. D. (2006). Effect of temperature and power frequency on milk fouling in an ohmic heater. *Food and Bioproducts Processing*, 84(4), 286–291.

Baaijens, F. P., Hulsen, M. A., & Anderson, P. D. (2004). The use of mixed finite element methods for viscoelastic fluid flow analysis. *Encyclopedia of computational mechanics*, 481-498.

Cappato, L. P., Ferreira, M. V., Guimaraes, J. T., Portela, J. B., Costa, A. L., Freitas, M. Q., Cunha, R.L., Oliveira, C.A.F., Mercali, G.D., Marzack, L.D.F., Cruz, A.G. (2017). Ohmic heating in dairy processing: Relevant aspects for safety and quality. *Trends in Food Science & Technology*, 62, 104–112.

De Alwis, A.d., & Fryer, P. (1990). The use of direct resistance heating in the food industry. *Journal of Food Engineering*, 11, 3-27.

de Souza, P. M., & Fernández, A. (2011). Effects of UV-C on physicochemical quality attributes and *Salmonella enteritidis* inactivation in liquid egg products. *Food Control*, 22(8), 1385–1392.

Dev, S. R. S., Raghavan, G. S. V., & Gariepy, Y. (2008). Dielectric properties of egg components and microwave heating for in-shell pasteurization of eggs. *Journal of Food Engineering*, 86(2), 207–214.

EFSA & ECDC, European Food Safety Authority & European Centre for Disease Prevention and Control (2011). The European Union summary report on trends and sources of zoonoses, zoonotic agents and food-borne outbreaks in 2009. EFSA Journal, 9(3), 2090, 378 pp.

Guo, W., Llave, Y., Jin, Y., Fukuoka, M., & Sakai, N. (2017). Mathematical modeling of ohmic heating of two-component foods with non-uniform electric properties at high frequencies. *Innovative Food Science and Emerging Technologies*, 39, 63–78.

Goullieux, A., & Pain, J. (2005). Ohmic heating. *Emerging technologies for food*, 469-505.

Horn, C. S., Franke, M., Blakemore, F. B., & Stannek, W. (1997). Modelling and simulation of pasteurization and staling effects during tunnel pasteurization of bottled beer. *Food and Bioproducts Processing*, 75(1), 23-33.

Huang, E., Mittal, G. S., & Griffiths, M. W. (2006). Inactivation of *Salmonella enteritidis* in liquid whole egg using combination treatments of pulsed electric field, high pressure and ultrasound. *Biosystems Engineering*, 94(3), 403–413.

Jaeger, H., Roth, A., Toepfl, S., Holzhauser, T., Engel, K. H., Knorr, D., Vogel, R.F., Bandick, N., Kulling, S., Heinz, V., Steinberg, P. (2016). Opinion on the use of ohmic heating for the treatment of foods. *Trends in Food Science & Technology*, 55, 84–97.

Jin, Y., Cheng, Y. D., Fukuoka, M., & Sakai, N. (2015). Electrical conductivity of yellowtail (*Seriola quinqueradiata*) fillets during ohmic heating. *Food and Bioprocess Technology*, 8(9), 1904–1913.

Knirsch, M. C., Dos Santos, C. A., Vicente, A., & Penna, T. C. V. (2010). Ohmic heating–a review. *Trends in Food Science & Technology*, 21(9), 436–441.

Koç, M., Koç, B., Susyal, G., Yilmazer, M. S., Ertekin, F. K., & Bağdatlıoğlu, N. (2011). Functional and physicochemical properties of whole egg powder: effect of spray drying conditions. *Journal of Food Science and Technology*, 48(2), 141–149.

Llave, Y., Fukuda, S., Fukuoka, M., Shibata-Ishiwatari, N., & Sakai, N. (2018). Analysis of color changes in chicken egg yolks and whites based on degree of thermal protein denaturation during ohmic

heating and water bath treatment. *Journal of Food Engineering*, 222, 151–161.

Llave, Y., Udo, T., Fukuoka, M., & Sakai, N. (2018b). Ohmic heating of beef at 20 kHz and analysis of electrical conductivity at low and high frequencies. *Journal of Food Engineering*, 228, 91–101.

Li, X., Sheldon, B. W., & Ball, H. R. (2005). Thermal resistance of *Salmonella enterica serotypes*, *Listeria monocytogenes*, and *Staphylococcus aureus* in high solids liquid egg mixes. *Journal of Food Protection*, 68(4), 703–710.

Lagunas-Solar, M. C., Zeng, N. X., Essert, T. K., Truong, T. D., Pina, C., Cullor, J. S., ... & Larraín, R. (2005). Disinfection of fishmeal with radiofrequency heating for improved quality and energy efficiency. *Journal of the Science of Food and Agriculture*, 85(13), 2273-2280.

Marra, F., Zell, M., Lyng, J. G., Morgan, D. J., & Cronin, D. A. (2009). Analysis of heat transfer during ohmic processing of a solid food. *Journal of Food Engineering*, 91(1), 56–63.

Mercali, G. D., Schwartz, S., Marczak, L. D. F., Tessaro, I. C., & Sastry, S. (2014). Ascorbic acid degradation and color changes in acerola pulp during ohmic heating: Effect of electric field frequency. *Journal of Food Engineering*, 123, 1–7.

Monfort, S., Mañas, P., Condón, S., Raso, J., & Álvarez, I. (2012a). Physicochemical and functional properties of liquid whole egg treated by the application of pulsed electric fields followed by heat in the presence of triethyl citrate. *Food Research International*, 48(2), 484–490.

Monfort, S., Saldaña, G., Condón, S., Raso, J., & Álvarez, I. (2012b). Inactivation of *Salmonella spp.* in liquid whole egg using pulsed electric fields, heat, and additives. *Food Microbiology*, 30(2), 393–399.

Monfort, S., Ramos, S., Meneses, N., Knorr, D., Raso, J., & Álvarez, I. (2012c). Design and evaluation of a high hydrostatic pressure combined process for pasteurization of liquid whole egg. *Innovative Food Science and Emerging Technologies*, 14, 1–10.

Nemeth, C. S., Friedrich, L., Pásztor-Huszár, K., Pipoly, E., Suhajda, Á., & Balla, Cs. (2011). Thermal destruction of *Listeria monocytogenes* in liquid egg products with heat treatment at lower temperature and longer than pasteurization. *African Journal of Food Science*, 5(3), 161–167.

Nakai, T., Kami, N., Fukuoka, M., & Sakai, N. (2018). Ohmic heating behavior of whole egg and measurement of electrical conductivity of egg constituents. *Japan Journal of Food Engineering*, 19(4), 199–207 (in Japanese).

Perry, J. J., Rodriguez-Saona, L. E., & Yousef, A. E. (2011). Quality of shell eggs pasteurized with heat or heat-ozone combination during extended storage. *Journal of Food Science*, 76(7), S437–S444.

Stefanou, G. (2009). The stochastic finite element method: past, present and future. *Computer methods in applied mechanics and engineering*, 198(9-12), 1031-1051.

Sakr, M., & Liu, S. (2014). A comprehensive review on applications of ohmic heating (OH). *Renewable and Sustainable Energy Reviews*, 39, 262-269.

Stadelman, W. J., Newkirk, D., & Newby, L. (1995). *Egg science and technology* (4th ed.). CRC Press.

Seyhun, N., Ramaswamy, H. S., Zhu, S., Sumnu, G., & Sahin, S. (2013). Ohmic tempering of frozen potato puree. *Food and Bioprocess Technology*, 6(11), 3200–3205.

Sánchez-Gimeno, A. C., Vercet, A., & López-Buesa, P. (2006). Studies of ovalbumin gelation in the presence of carrageenans and after manothermosonication treatments. *Innovative Food Science and Emerging Technologies*, 7(4), 270–274.

Shynkaryk, M. V., Ji, T., Alvarez, V. B., & Sastry, S. K. (2010). Ohmic heating of peaches in the wide range of frequencies (50 Hz to 1 MHz). *Journal of Food Science*, 75(7), E493–E500.

Wu, G. X., & Taylor, R. E. (2003). The coupled finite element and boundary element analysis of nonlinear interactions between waves and bodies. *Ocean Engineering*, 30(3), 387-400.

ARS, U.S. Department of Agriculture, Agricultural Research Service (1969). Egg pasteurization manual. ARS 74-78. U.S. Department of Agriculture, Agricultural Research Service, Albany, Calif. https://naldc.nal.usda.gov/download/CAIN709025458/PDF. Accessed May 28, 2021.

Code of Federal Regulations-CFR (2020). 9 CFR 590.570. U.S. Government Printing Office, Washington, D.C. https://www.govinfo.gov/app/details/CFR-2020-title9-vol2/CFR-2020-title9-vol2-sec590-570/summary. Accessed May 28, 2021.

CDC, Centers for Disease Control and Prevention Salmonella infections linked to Gravel ridge farms shell eggs (2018). https://www.cdc.gov/salmonella/enteritidis-09-18/index.html. Accessed May 28, 2021.

FAO, Food and Agriculture Organization of the United Nations (2021). Livestock Primary. http://www.fao.org/faostat/en/?#data/QL. Accessed May 28, 2021.

ORKA Food Technology. (2021) Nutrient Content of a Large Egg. https://eggtester.com/nutrition/. Accessed May 28, 2021.

Chapter 2 – Electrical conductivities analysis during ohmic heating

2.1 Introduction

One of the most important factors in ohmic heating study is the electrical conductivity (EC) of material, which could be affect by several factors, such as temperature, frequency, voltage, and concentration of electrolytes. The presence of ionic substances such as acids and salts could increase EC values, while the presence of non-polar constituents like fat and lipids would decrease them (Sakr & Liu, 2014). Many studies have reported that the EC of materials had linear relationship with temperature in a certain temperature range, for example, Darvishi et al. (2012) reported that the EC of liquid egg samples (including egg white, egg yolk, and whole egg) increased linearly with the rise of temperature in the range of 19 to 60 ℃ during OH (150 V and 60 Hz). The same linear relationship between EC with temperature during OH (50 V, 50 and 20000 Hz) was also reported by Nakai et al (2018) in the temperature range of 10 to 70 ℃.

However, the linear relationship between EC and temperature is not always observed at high temperature. Several authors have reported that high temperatures may favor the formation and expansion of air bubbles inside the food, leading to a reduction of the electrical conductivity (Castro et al., 2004). In addition to the presence of air bubbles (gas), the gradual boiling of water molecules increase solids concentration, reducing ions mobility (Castro et al., 2004, Darvishi et al., 2013, Sarang et al., 2008).

Since biological objects are sensitive to electric fields, current flow becomes nonlinear with respect to voltage. Moreover, the voltage applied to the electrodes where this nonlinearity becomes important depends on frequency. While at a low frequency, just a few millivolts can induce changes in the electrical properties of the object, several volts may be needed at high frequencies (Pliquett, 2010). Impedance characterizes how an object alters current flow due to an outer electric field (Krassen et al., 2007). In an alternating current circuit, the overall resistance to current can change quite dramatically with frequency, and is more accurately described by resistance (R) than by impedance (Z_e) (Liu et al., 2017). And the electrical impedance and resistance (used to calculate the EC) of food samples under different frequencies during OH have been studied in many studies, of which the results showed that the impedance and resistance have significant difference under low frequencies but the two values got almost same when frequency was high. For example, Liu et al. (2017) reported that the impedance and resistance of tuna during OH thawing have no significant different when the frequency over 1000 Hz in the temperature range of -5 to 20 ℃. And the same phenomenon was also reported in the studies of beef (Llave et al., 2018a) and liquid eggs (Nakai et al., 2018) during OH, the impedance (Z_e) and resistance (R) showed significant difference in the frequency

range of 50 to 500 Hz, and the values of Z_e and R became same when the frequency over 500 Hz in the temperature range of 5 to 65 ℃. That is because the capacitive reactance dominates at low frequencies but approaches zero at high frequencies (Sastry & Kamonpatana, 2014). And only the electrical resistance (R) of liquid egg samples were used for EC analysis during OH (20 kHz) in this study for this reason.

2.2 Materials and Methods

2.2.1 Samples preparation

The fresh raw eggs used in this study were obtained from a Japanese department store shown in **Table 2-1**.

Table 2-1 Hen eggs used in this study

Product name	Abukuma Kogen Eggs
Place of purchase	Queens Isetan Shinagawa store
Production place	Sakai Chicken Farm Karukome-39 Yamashiraishi, Asakawa, Ishikawa District, Fukushima 963-6203
Egg type	White shell
Egg size	66 ± 1.4 g

Whole liquid eggs were stirred using a homogenizer (PT10-35GT; KINEMATICA AG Co. Ltd., Switzerland) at 5,000 rpm for 100 s at room temperature (20 °C) and sifted using an appropriate stainless steel sieve to remove the chalazae and yolk membranes. Then, liquid whole egg samples were collected for OH. To obtain liquid egg samples, the egg whites were stirred using a homogenizer at 5,000 rpm for 100 s, while the egg yolks were sieved using an appropriate stainless steel sieve to remove the chalazae and yolk membranes. These three samples were stored in a controlled temperature chamber at 20 °C for no more than 4 h before the experiments. And the liquid egg samples preparation method flow is shown by **Fig. 2-1**.

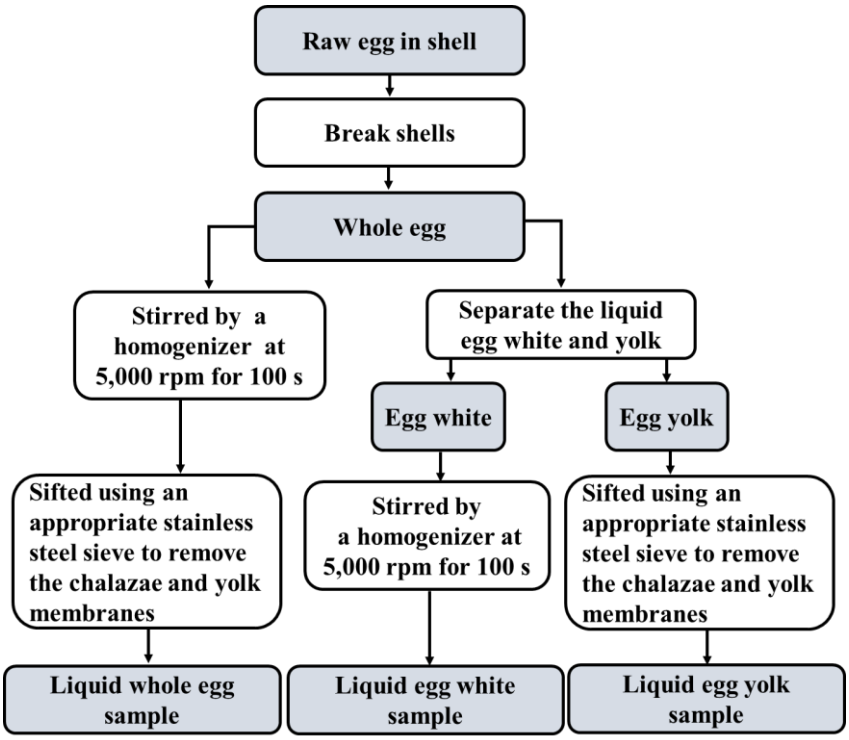

Fig. 2-1 Liquid egg samples preparation method flow

2.2.2 Electrical conductivities acquisition during OH

The OH system consisted of a polystyrene chamber (internal size of 4 × 4 × 4 cm3 and 2.5-cm thick walls), which was filled with a single liquid egg (64.37 ± 0.22 g, 63.16 ± 0.52, or 63.07 ± 0.69 g of egg white, egg yolk, or whole egg, respectively), two titanium plate electrodes (4 cm wide, 10 cm high, and 0.01 cm thick) facing each other at opposite ends of the chamber (**Fig. 2-2**), an alternating current power supply, and a control panel for controlling the voltage. A constant voltage of 50 V was applied to the electrodes using a Joule heating machine (FJB-5.5, Frontier Engineering Co. Ltd., Japan) at a frequency of 20 kHz.

An OH process was conducted to raise the sample temperature from 20 °C until the temperature at the hot spot achieved the target temperature at which the thermal protein denaturation began, which was 59.1 °C for the egg white and whole egg and 63.3 °C for the egg yolk (Llave et al., 2018b) to avoid thermal protein denaturation of liquid eggs. An amperemeter and a voltmeter (Digital Multimeter DT4282; HIOKI, Japan) were connected to the OH system to measure the current and voltage during the OH process. A personal computer and a temperature-measuring system (FTC-DIN-ST-TH, Photon Control, Canada) were used to collect the center temperature, current, and voltage data at intervals of 1 s (**Fig. 2-2**).

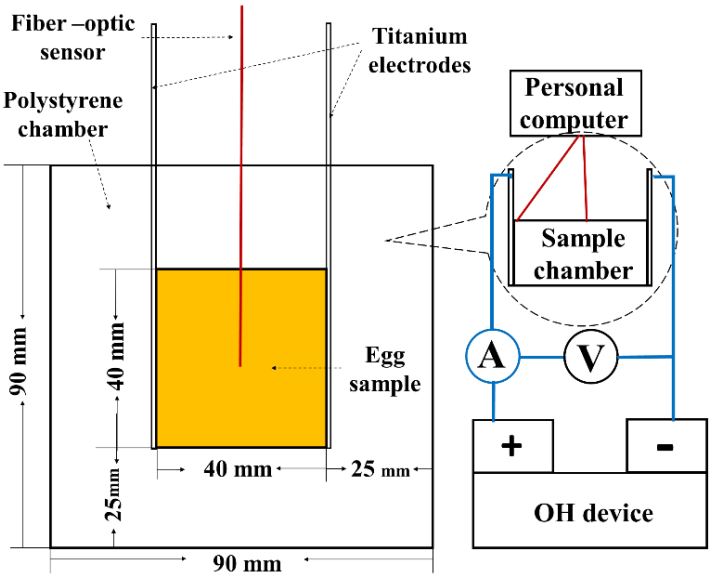

Fig. 2-2 Schematic diagram of the central vertical cross-section of the ohmic heating system

The EC values (σ) of liquid egg samples during OH at 20 kHz and a temperature range of 20 °C–63.3 °C were calculated using **Eq. (1)**:

$$\sigma = \frac{I}{U} \times \frac{L}{A} \qquad (1)$$

where σ, I and U are the electrical conductivity ($S \cdot m^{-1}$),current (A) and voltage (V) of the samples, respectively, L is the distance between the two electrode plates (m), and A is the area of the sample connected to the electrode plate (m^2).

The relationship between EC and the temperature of the liquid eggs was obtained for further computer simulation studies (**Chapter 4**). The center temperature of the liquid egg samples was used to build this relationship.

2.3 Results and Discussion

The relationship between EC and the center temperature of the evaluated liquid egg samples is shown in **Fig. 2-3**. The EC results of the liquid egg samples showed a good linear relationship with temperature, and these EC values increased linearly with increasing temperature in the evaluated range, which because of the increasing of ionic mobility during OH due to the structural changes in the tissue like cell wall protopectin breakdown (Darvishi et al., 2012).

The EC values of egg yolk and white were the smallest and the largest, respectively, while the EC values

for whole eggs were between them. The related equations are summarized in **Chapter 4** for computer simulation. The difference of EC among liquid egg white, whole egg, and egg yolk at the same temperature maybe because of the chemical composition differences of them. For example, liquid egg had the highest water content and lowest fat content, which made it have the largest EC due to the highest ionic mobility among the liquid egg samples during OH. On the other hand, liquid egg yolk, which had the lowest water content and highest fat content showed the smallest EC among liquid egg samples during OH (Darvishi et al., 2012).

And the of EC of liquid egg white (0.75-1.41 $S \cdot m^{-1}$, in the temperature range of 20 to 59 ℃), whole egg (0.49-0.92 $S \cdot m^{-1}$, in the temperature range of 20 to 59 ℃), and egg yolk (0.26-0.54 $S \cdot m^{-1}$, in the temperature range of 20 to 63 ℃) during OH at 50 V and 20 kHz are consistent with the results previously reported by Nakai et al. (2018), in which show the EC values of liquid egg white (around 0.79 and 1.45 $S \cdot m^{-1}$ at 20 and 60 ℃, respectively), whole egg (around 0.58 and 1.05 $S \cdot m^{-1}$ at 20 and 60 ℃, respectively), and egg yolk (around 0.28 and 0.50 $S \cdot m^{-1}$ at 20 and 60 ℃, respectively) at 50 V and 20 kHz.

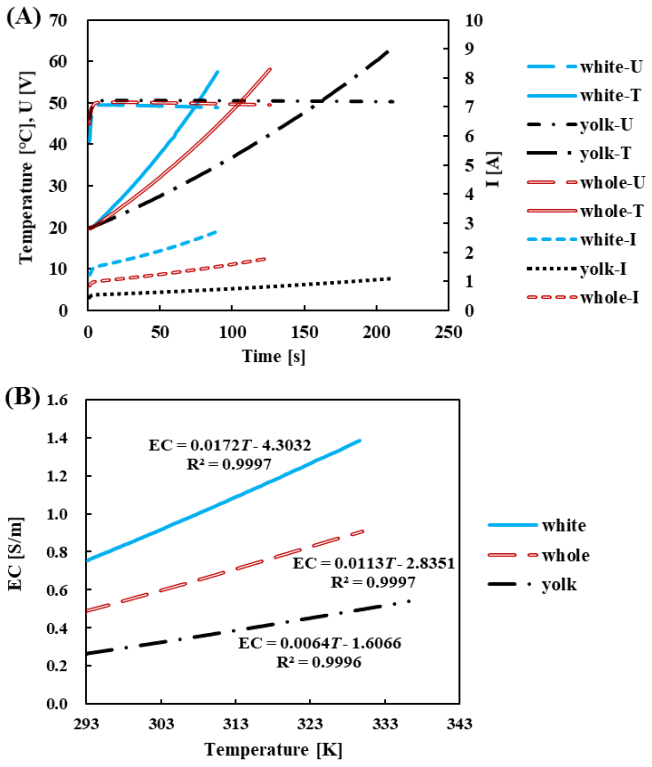

Fig. 2-3 Voltage (U), current (I), and center temperature (T) of liquid egg samples (A), and the relationship between electrical conductivity (EC) and the center temperature (B) of liquid egg samples during OH (20 kHz and 50 V).

2.4 Conclusions

The EC results of the liquid egg samples showed a good linear relationship with temperature, and these EC values increased linearly with increasing temperature in the evaluated temperature range (20 °C–63.3 °C). The EC values of egg yolk and white were the smallest and the largest, respectively, while the EC values for whole eggs were between them during OH.

2.5 References

Castro, I., Teixeira, J. A., Salengke, S., Sastry, S. K., & Vicente, A. A. (2004). Ohmic heating of strawberry products: electrical conductivity measurements and ascorbic acid degradation kinetics. *Innovative Food Science & Emerging Technologies*, 5(1), 27-36.

Darvishi, H., Khostaghaza, M. H., & Najafi, G. (2013). Ohmic heating of pomegranate juice: Electrical conductivity and pH change. *Journal of the Saudi Society of Agricultural Sciences*, 12(2), 101-108.

Darvishi, H., Khoshtaghaza, M. H., Zarein, M., & Azadbakht, M. (2012). Ohmic processing of liquid whole egg, white egg and yolk. Agricultural Engineering International: *CIGR Journal*, 14(4), 224-230.

Nakai, T., Kami, N., Fukuoka, M., & Sakai, N. (2018). Ohmic heating behavior of whole egg and measurement of electrical conductivity of egg constituents. *Japan Journal of Food Engineering*, 19(4), 199–207 (in Japanese).

Liu, L., Llave, Y., Jin, Y., Zheng, D. Y., Fukuoka, M., & Sakai, N. (2017). Electrical conductivity and ohmic thawing of frozen tuna at high frequencies. *Journal of Food Engineering*, 197, 68-77.

Llave, Y., Udo, T., Fukuoka, M., & Sakai, N. (2018). Ohmic heating of beef at 20 kHz and analysis of electrical conductivity at low and high frequencies. *Journal of food engineering*, 228, 91-101.

Llave, Y., Fukuda, S., Fukuoka, M., Shibata-Ishiwatari, N., & Sakai, N. (2018b). Analysis of color changes in chicken egg yolks and whites based on degree of thermal protein denaturation during ohmic heating and water bath treatment. *Journal of Food Engineering*, 222, 151–161.

Sastry, S. K., & Kamonpatana, P. (2014). Electrical conductivity of foods. In M. A. Rao, S. S. H. Rizvi, A. K. Datta, & J. Ahmed (Eds.), *Engineering properties of foods* (pp. 527–570). Fourth Edition, Boca Raton, FL: CRC Press, Taylor & Francis Group.

Sarang, S., Sastry, S. K., & Knipe, L. (2008). Electrical conductivity of fruits and meats during ohmic heating. *Journal of Food Engineering*, 87(3), 351-356.

Sakr, M., & Liu, S. (2014). A comprehensive review on applications of ohmic heating (OH). *Renewable and Sustainable Energy Reviews*, 39, 262-269.

Chapter 3 – Temperature, pasteurization effect and quality analysis during ohmic heating pasteurization

3.1 Introduction

The heating is generated directly in the materials tough the conversion of electric energy into thermal during OH, and it is well known as a volumetric heating method that offers better temperature uniformity than traditional methods. However, temperature non-uniformity could be observed during OH even the materials had uniform EC, the key parameter influencing the heating rate of OH (Goullieux & Pain, 2005; Marra et al., 2009).

The principal mechanism of microbial inactivation during the OH process is thermal in nature (Knirsch et al., 2010), and the temperature profiles in cold spots must be sufficient to inactivate pathogens (Cappato et al., 2017). In this study, the leading common pathogen in contaminated egg products, *Salmonella typhimurium*, of which the slope of the thermal destruction-time curve for liquid egg white, whole egg, and egg yolk were 4.2, 4.3, and 4.4, respectively (Garibaldi et al., 1969), and the required pasteurization temperature were 54, 58, 59 °C for liquid egg white, whole egg, and egg yolk, respectively for at least 10 min pasteurization processing (MHLW, 1959) was treated as the target pathogen, because the outbreaks of diseases caused by *Salmonella* infection in raw eggs continue to pose a public health threat (CDC, 2018; EFSA & ECDC, 2011; Mukhopadhyay & Ramaswamy, 2012). On the other hand, hot spots during thermal processing have been considered as a critical point for food quality (Jaeger et al., 2016), which should be given priority to avoid the quality change of food materials caused by local overheating during processing.

The changes in physicochemical properties and quality attributes of egg products due to the application of thermal process have also been reported in the literature, such as color (Koç et al., 2011; Llave et al., 2018), viscosity (Sánchez-Gimeno et al., 2006), emulsifying properties (Monfort et al., 2012), and foaming and gelling properties (Alamprese et al., 2019). From these changes, color is one of the most studied attributes because egg color affects the acceptability of many egg-based products. However, most of these changes have been related to the non-homogeneous degree of thermal protein denaturation, which varies depending on the target component in the egg. However, to the best of our knowledge, the relationship between the degree of pasteurization and the thermal protein denaturation of liquid eggs has not been studied in detail for OH applications at high frequencies, to assure not only quality retention but also food safety.

In this study, liquid egg samples were OH-treated (including OH and thermal keep approaches) at 20

kHz from room temperature to the target temperature with the aim of effectively pasteurizing the sample and to attempt high-quality attribute retention, focusing on thermal protein denaturation and color changes.

3.2 Materials and Methods

3.2.1 Materials

The sample preparation methods are same as **Chapter 2.**

3.2.2 Temperature measurement during pasteurization

The OH system consisted of a polystyrene chamber (internal size of 4 × 4 × 4 cm^3 and 2.5-cm thick walls), which was filled with a single liquid egg (64.37 ± 0.22 g, 63.16 ± 0.52, or 63.07 ± 0.69 g of egg white, egg yolk, or whole egg, respectively), two titanium plate electrodes (4 cm wide, 10 cm high, and 0.01 cm thick) facing each other at opposite ends of the chamber (**Fig. 3-1**), an alternating current power supply, and a control panel for controlling the voltage. A constant voltage of 50 V was applied to the electrodes using a Joule heating machine (FJB-5.5, Frontier Engineering Co. Ltd., Japan) at a frequency of 20 kHz. The experimental heating process included two approaches. In the first approach, an OH process was conducted to raise the sample temperature from 20 °C until the temperature at the hot spot achieved the target temperature at which the thermal protein denaturation began, which was 59.1 °C for the egg white and whole egg and 63.3 °C for the egg yolk (Llave et al., 2018). In the second approach, an additional thermal keeping process was included, where samples were kept inside the thermal insulation chamber to finalize the pasteurization process using the residual temperature (the cold spot temperature was used as the target). The results represent the average of three samples.

Two fiber-optic sensors (1.6 mm diameter) were placed at the center and top corner (identified by the coordinates in space of 0, 0, 0 cm and 2, 2, and 2 cm, respectively) of the liquid egg samples to monitor their internal temperatures. These positions were assumed as the hot and cold spots, respectively. A personal computer and a temperature-measuring system (FTC-DIN-ST-TH, Photon Control, Canada) were used to collect the temperature, data at intervals of 1 s (**Fig. 3-1**).

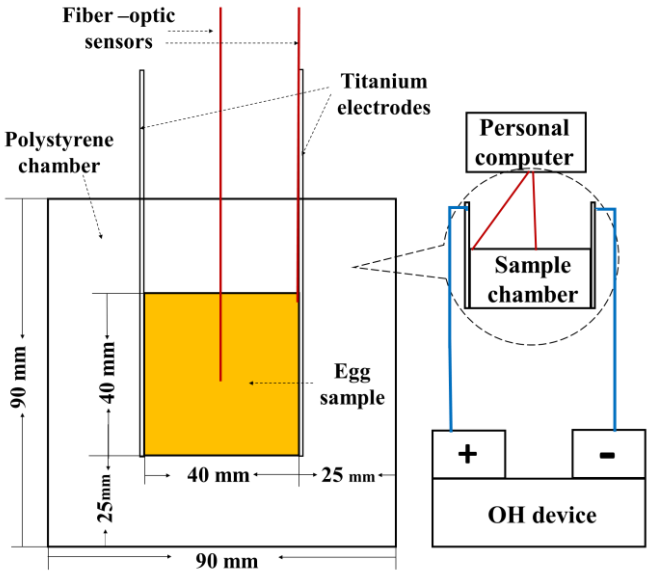

Fig. 3-1 Schematic diagram of the central vertical cross-section of the ohmic heating system

3.2.3 Pasteurization effect evaluation

The thermal pasteurization standard of liquid egg samples referred the pasteurization standards of the Japanese Ministry of Health, Labor, and Welfare (MHLW, 1959), as **Table 3-1** showing:

Table 3-1 Pasteurization standard of liquid eggs

	Continuous pasteurization		Batch pasteurization	
	Temperature (℃)	Time (min)	Temperature (℃)	Time (min)
Whole egg	60		58	
Egg yolk	61	3.5	59	10
Egg white	56		54	

Thermal pasteurization process including continuous and batch pasteurization (Takano & Kashiyama, 1998). Continuous pasteurization is the rapid transfer of heat to medium through steam condensate without the use of a heat exchanger. On the other hand, during batch pasteurization, the entire volume of media is pasteurized at once through the use of thermal techniques, which including 3 steps: heating, holding, and cooling. The batch pasteurization standard of MHLW (1959) is used as the reference because the pasteurization processing matched with this study, and the thermal pasteurization effect of the heating

process was evaluated using the pasteurization value (*P*-value), calculated using Eq. (1):

$$P = \int 10^{\frac{T - T_{ref}}{Z_t}} dt \quad (1)$$

where t is the heating time (min), T is the temperature of the sample (°C), T_{ref} is the standard temperature of liquid eggs for pasteurization (°C), and Z_{t} is the slope of the thermal destruction-time curve (°C) for a standard reference strain of *Salmonella typhimurium*. The T_{ref} values were selected based on the standard values defined by the Japanese Ministry of Health, Labor, and Welfare as 54 °C, 58 °C, and 59 °C for egg white, whole egg, and egg yolk, respectively (MHLW, 1959). The Z_{t} values used in Eq. (2) were 4.2 °C, 4.3 °C, and 4.4 °C for liquid egg white, whole egg, and egg yolk, respectively (Garibaldi et al., 1969).

3.2.4 Thermal protein non-denaturation evaluation

Many physicochemical and functional properties of food products were related to the protein state. And the thermal protein degree of food materials was a key factor for quality evaluation. Although thermal protein denaturation is a complicated process involving more than 1 intermediate state of a protein of interest, a 2-state model assuming native (N) and denatured (D) molecular states is often employed in rate analysis for the sake of simplicity (Villota and Hawkes, 2007):

$$\mathrm{N} \rightarrow \mathrm{D} \quad (2)$$

If this reaction followed first-order reaction kinetics, the change in the fraction of native molecules during heating can be described as follows:

$$\frac{d}{dt}\left(\frac{C_{it}}{C_{i0}}\right) = \frac{dX_i}{dt} = -k_{ti}(T)X_i \quad i = 1,2 \quad (3)$$

where t is the time (min), k_{ti} is the reaction rate constant ($\mathrm{min^{-1}}$), and the subscripts (i = 1 and 2) represent the respective protein (ovalbumin for egg white and whole egg, or low-density lipoproteins for egg yolk) in the evaluated range (Llave et al., 2018). The rate constant k_{ti} is a function of temperature, and it can be determined at any time if a time-temperature profile is available. Moreover, C_{i0} and C_{it} are the concentrations of non-denatured protein at the initial state and at time t, respectively, and X_i represents C_{it}/C_{i0}, as the non-denaturation ratio.

The temperature dependence of the reaction rate constant is assumed to follow the Arrhenius equation:

$$k_{ti} = Z_i \, exp\left(-\frac{E_{ai}}{R_t T}\right) \quad i = 1,2 \quad (4)$$

where Z_i is the pre-exponential factor ($\mathrm{min^{-1}}$), E_{ai} is the activation energy of denaturation ($\mathrm{kJ \cdot mol^{-1}}$), R_{t} is the gas constant ($\mathrm{J \cdot K^{-1} mol^{-1}}$), and T is the absolute temperature (K). The Z_i and E_{ai} values were reported in

a previous study (Llave et al., 2018).

3.2.5 Color analysis of liquid egg samples

Egg color affects the acceptability of many egg-based products. Color perception depends strongly on the chemical and physical properties of the egg components (Min et al., 2005). The color of egg yolk is attributed to fat-soluble carotenoids (xanthophylls; including lutein, zeaxanthin, β-cryptoxanthin and minor amounts β-carotene) (Li-Chan and Kim, 2008). Laca et al. (2010) reported that the yolk pigments appeared mainly in the lipidic paste obtained from the plasma of egg yolk, where the lipids are concentrated. In the case of egg white, it has been reported that denaturation of certain proteins, which occurs due to thermal coagulation, explains the main color changes in samples, translucency and/or opacity, depending on the applied treatment (Su and Lin, 1993). However, color of liquid eggs was an important for quality evaluation.

The images of liquid egg samples before processing, after OH (approach 1), and after OH plus thermal keep approaches (approaches 1 and 2) were obtained, and the changes in sample color were estimated via computer vision system (CVS) using the method described in previous studies (Llave et al., 2017a, b) with some modifications (**Fig. 3-2**):

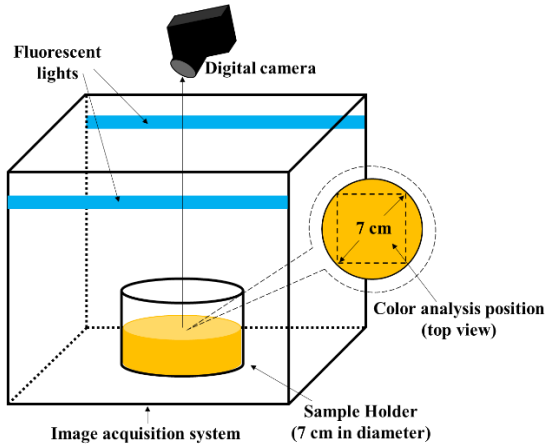

Fig. 3-2 The image acquisition system for color analysis

(1) Lighting system: Two lamps (60 cm long), each consisting of a fluorescent tube (FL20S.D-EDL-D65, natural daylight, 21 W; Toshiba Lighting and Technology, Japan) with a color temperature of 6,500 K

(D65; the standard light source commonly used in food research) were placed facing each other to illuminate the samples.

(2) Sample holder: A transparent PVC cylinder container (7.0 cm internal diameter), placed over a black PVC board was used as the sample holder for image acquisition.

(3) Digital camera and image acquisition: a color digital camera (D5100; Nikon, Japan) with a lens (AF-SDX Nikkor 18-105 mm f/3.5-5.6G ED VR; Nikon) was placed over the sample holder inside the imaging acquisition apparatus, which was placed in a dark room. The conditions of the camera were set as follows: manual mode with a lens aperture *F* of 4.5, a shutter speed of 1/125, a zoom of 32 mm, and no flash.

(4) Image pre-processing: The images were cropped to separate the sample (88×88 pixels) from the background using Microsoft PowerPoint.

(5) Color acquisition via CVS: CVS was used to estimate the changes in the color of the samples from the captured digital images. A transformation approach of color space was used to convert R′G′B′ values into L^* (lightness), a^* (redness), and b^* (yellowness) values, as described by Mendoza et al. (2006):

The nonlinear R′G′B′ values are transformed to linear sRGB (Standard *RGB*) , which is defined by the International Electrotechnical Commission (IEC) as IEC 61966-2-1 (1999) as an international color standard. And the transforms are calculated by Eqs (6-7).

If R', G', $B' \leq 0.04045$

$$sR = \frac{R'}{12.92}\ ,\ sG = \frac{G'}{12.92}\ ,\ sB = \frac{B'}{12.92} \tag{6}$$

else if R', G', $B' > 0.04045$

$$sR = -\left(\frac{-R'+0.055}{1.055}\right)^{2.4},\ sG = -\left(\frac{-G'+0.055}{1.055}\right)^{2.4}\ ,\ sB = -\left(\frac{-B'+0.055}{1.055}\right)^{2.4} \tag{7}$$

Then, using the recommended coefficients by the Rec. ITU-R BT.709-5 (2002), *sRGB* color space values are converted to the CIE *XYZ* color space system by Eq. (8).

$$\begin{bmatrix} X \\ Y \\ Z \end{bmatrix} = \begin{bmatrix} 0.4124 & 0.3576 & 0.1805 \\ 0.2126 & 0.7152 & 0.0722 \\ 0.0193 & 0.1192 & 0.9505 \end{bmatrix} \begin{bmatrix} sR \\ sG \\ sB \end{bmatrix} \tag{8}$$

In the *R′G′B′* encoding process, the power function with a gamma factor of 2.4 includes a slight black-level offset to allow for the invertibility in integer math, which closely fits a straightforward gamma 2.2 curve. Therefore, consistency was maintained using the gamma 2.2 legacy images and the video industry (Mendoza et al., 2006). Also, the *sRGB* tristimulus values <0.0 or >1.0 were rounded to

0.0 and 1.0, respectively.

Color spaces: In food research, color is often represented using the *L* a * b** color space. The definition of *L* a * b** is based on the intermediate system, CIE *XYZ*, which simulates the human perception (Rec. ITU-R BT. 709-5, 2002) and may be converted from the *RGB*, as shown in Eq. (8). Thus, *L* a * b** is defined as follows:

*L** is the luminance or lightness component that goes from 0 (black) to 100 (white), and parameters *a ** (from green to red) and *b** (from blue to yellow) are the two chromatic components, varying from −120 to +120. The definition of L* *a* *b* is based on the intermediate system CIE *XYZ* which simulates the human perception (Rec. ITU-R BT. 709-5, 2002) and which may be converted from RGB, as showed in Eq. (8). Thus, *L**, *a**, and *b** are defined as

$$L^* = 116f\left(\frac{Y'}{Y'_n}\right) - 16 \qquad (9)$$

$$a^* = 500[f\left(\frac{X'}{Y'_n}\right) - f\left(\frac{Y'}{Y'_n}\right)] \qquad (10)$$

$$b^* = 200[f\left(\frac{Y'}{Y'_n}\right) - f\left(\frac{Z'}{Z'_n}\right)] \qquad (11)$$

where

$$f(q) = \begin{cases} q^{1/3} & if\ q > 0.008856 \\ 7.787q + \frac{16}{116} & otherwhise \end{cases} \qquad (12)$$

X'_n, Y'_n, and Z'_n are the tristimulus values of the perfect diffuse white surface (95.043, 100.000, 108.879, respectively) for the standard illuminant, D65.

(6) Color value change calculation

The changes in the color of the liquid egg samples were calculated using **Eqs. (13-17)**, considering the values before and after heating.

$$\Delta L^* = L^*_{after\ heating} - L^*_{before\ heating} \qquad (13)$$

$$\Delta a^* = a^*_{after\ heating} - a^*_{before\ heating} \qquad (14)$$

$$\Delta b^* = b^*_{after\ heating} - b^*_{before\ heating} \qquad (15)$$

$$\Delta E^* = \sqrt{\Delta L^{*2} + \Delta a^{*2} + \Delta b^{*2}} \qquad (16)$$

$$\Delta C^* = \sqrt{\Delta a^{*2} + \Delta b^{*2}} \qquad (17)$$

where ΔE^* is the total color difference and ΔC^* is the difference in chroma (color saturation).

3.2.6 Statical analysis

The data were analyzed via one-way analysis of variance (ANOVA) using Microsoft Excel software. Differences were considered significant at $p < 0.05$.

3.3 Results and Discussion

3.3.1 Temperature analysis during processing

Temperature profiles of liquid egg samples at center and top-corner (assumed hot and cold spots, respectively) during OH (50 V and 20 kHz) and thermal keep approaches were shown in **Fig. 3-4**, which showed that the heating rate of egg white and yolk were the largest and smallest, respectively, while the heating rate od whole eggs were between them during OH. And the heating rate of liquid egg samples during OH was positively correlated with EC (shown in **Chapter 2**), which were consistent with the results reported by Darvishi et al. (2012) and Nakai et al. (2018). It took 90, 136, and 216 seconds of OH for liquid egg white, whole egg, and yolk samples, respectively to achieve target temperature (the center temperature of egg samples), and the temperature difference of the two location of each sample at that time was 26.9, 21.2, and 25.4 ℃, respectively. After stopping OH, the temperature differences between the two locations of liquid egg samples became smaller as the thermal keep approach went on, achieved 13.5, 10.4, and 15.3 ℃ for egg white, whole egg, and egg yolk, respectively at the end of heating processing (10 min, including OH and thermal keep approaches).

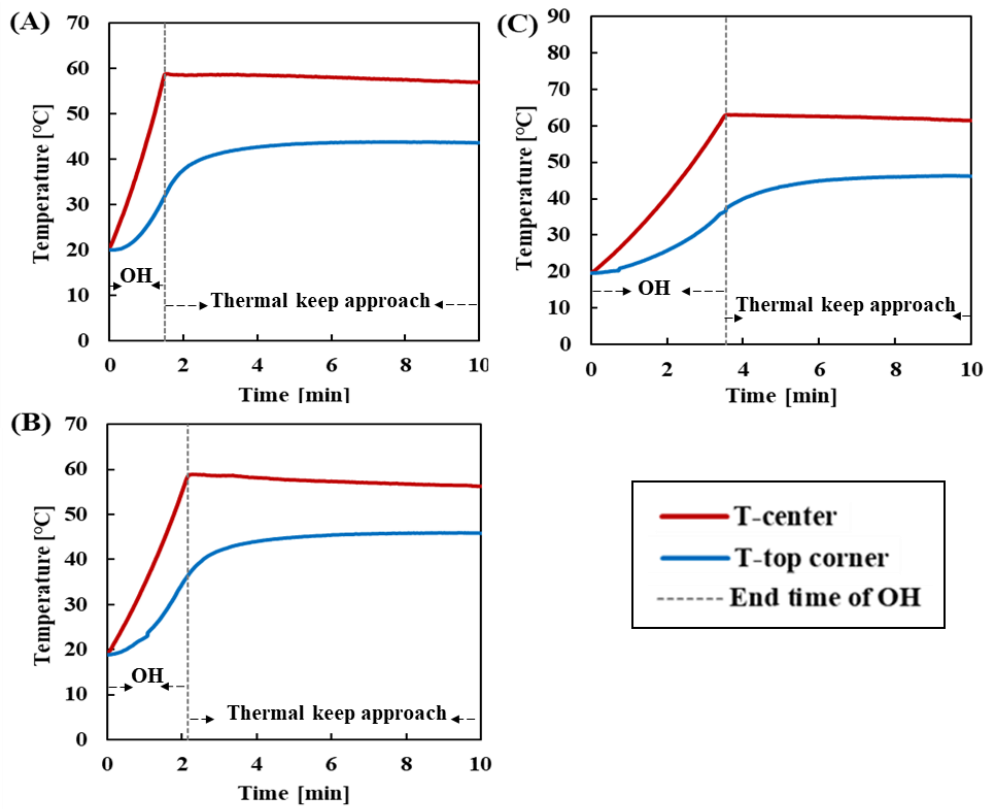

Fig. 3-4 Temperature profiles of egg white (A), whole egg (B), and egg yolk (C) samples during OH (20 kHz and 50 V) plus thermal keeping stage (approaches 1 and 2).

Although OH is well known as a volumetric method that offers better temperature uniformity than traditional methods, and the heating rate of materials during OH is highly depending on EC. The temperature profiles of liquid egg samples at center and top-corner in this study provided that large temperature difference would occur during OH even the materials had EC uniformity because of the thermal losses, owing to the contact between the sample and chamber. This could be because the top part of the electrodes was exposed to air during its connection to the heating machine; thus, the samples slightly lost heat to the air along the tangential direction, which caused a drop in the temperature of the top corner for all liquid egg samples.

A similar phenomenon was observed in the study of Marra et al. (2009), where the temperature within the sample (mashed potato) was uniform, but slightly cold regions were observed, owing to heat losses to the electrodes and chamber surfaces. These heat losses in the chamber surfaces (in contact with the sample) and electrodes have been reported to be critical for sterilization (including pasteurization) calculations (Jun & Sastry, 2007).

3.3.2 Pasteurization value, and *X* analysis during processing

Pasteurization effect of liquid egg samples were evaluated using thermal pasteurization value (*P*-value) calculated depending on the temperature profiles. The P-value profiles at the center (hot spot, T_h) and top corner (cold spot, T_c) of the three liquid egg samples during OH and the thermal keep approach are shown in **Fig. 3-5**. Although it can be observed that the center of egg white and yolk achieved the pasteurization standard (P-value above 10 min) after a short processing time, the *P*-values at the top corner remained at approximately 0 because the temperature it reached was not high enough. In the case of whole eggs, the pasteurization standard was not reached even at the center (T_h).

As one of the quality evaluation indexes of liquid egg samples in this study, thermal protein non-denaturation ratio (*X*) was also calculated depending on the temperature profiles.

The ovalbumin and low-density lipoproteins (LDL) began denaturing at 59.17 ℃ and 63.33 ℃ for egg white and egg yolk, respectively (Llave et al., 2018). For the whole egg samples, the denaturation degree was focused on ovalbumin (as in the case of egg white) because the temperature during the process (58 °C) did not reach the protein denaturation temperature of LDL.

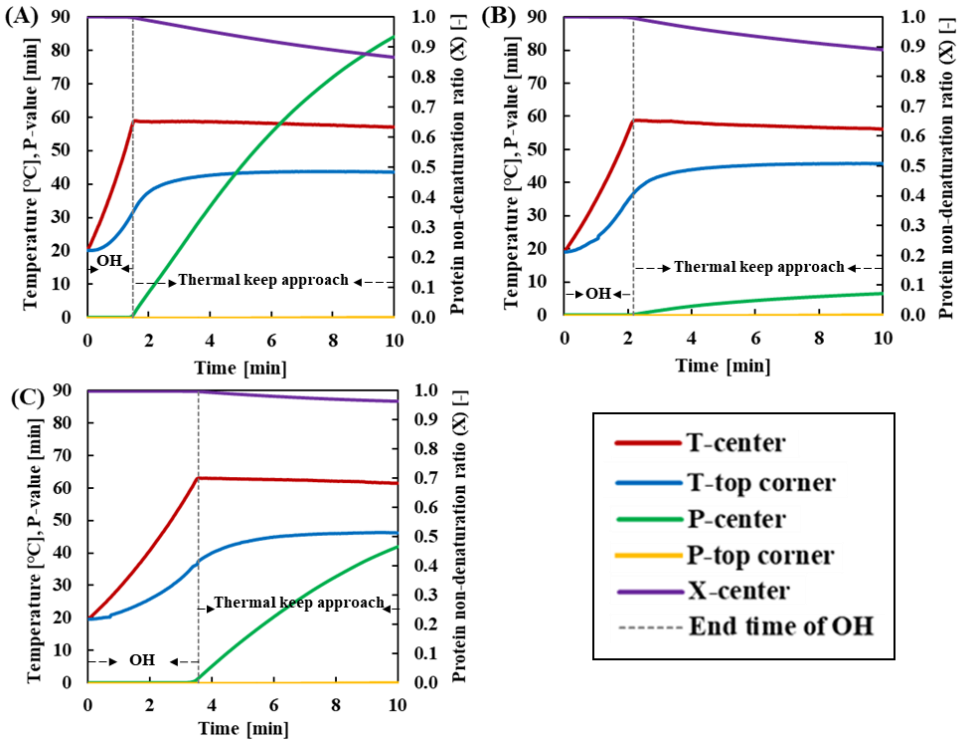

Fig. 3-5 Temperature, P-value, and protein non-denaturation ratio (*X*) profiles of egg white (A), whole egg (B), and egg yolk (C) samples during OH (20 kHz and 50 V) plus thermal keeping stage (approaches 1 and 2). T: temperature, P: P-value, *X*: protein non-denaturation ratio.

As shown in **Fig. 3-5** and **Table 3-2**, the degree of protein denaturation of liquid egg samples was evaluated using the protein non-denaturation ratio (X) under OH and thermal keep approaches. From the results, it can be concluded that liquid egg samples had nearly no protein denaturation after 10 min of processing (X values at hot spot were 0.87, 0.89, and 0.96 for egg white, whole egg, and egg yolk, respectively). It can be considered that the protein denaturation of egg samples was not severe, and the quality of the samples were almost retained even after processing. The degree of denaturation of the liquid whole egg was evaluated based on the egg white portion because this protein was more easily denatured than the yolk portion.

Table 3-2. Thermal protein non-denaturation ratio of liquid egg samples at the end of OH (approach 1) and OH plus thermal keep approach (approach 2)

Sample	Thermal protein non-denaturation ratio (X)	
	At the end of approach 1	At the end of approach 2
Egg white (ovalbumin)	0.99	0.87
Whole egg (ovalbumin)	0.99	0.89
Egg yolk (LDL)	0.99	0.96

3.3.3 Color change evaluation of liquid egg samples

The color of liquid egg samples was analyzed as the other index for quality evaluation in this study, and the images of liquid egg samples before processing, after OH only (approach 1), and after OH plus thermal keep approach (approaches 1 and 2) were shown by **Fig. 3-6**.

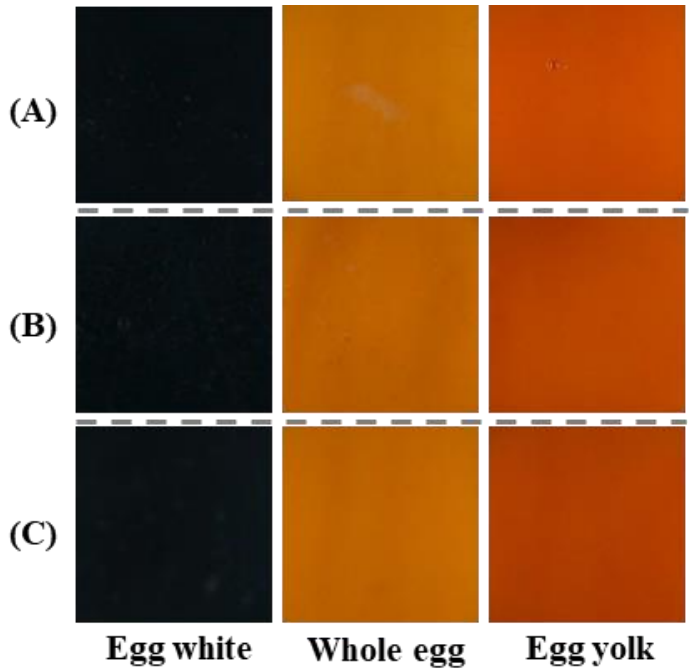

Fig. 3-6 Images of liquid egg samples before processing (A), after OH only (B), and after OH plus thermal keep approach (C) for color analysis.

The changes in the color of liquid eggs could not only be used to analyze the quality retention attributes directly via a sensory evaluation but could also reflect changes in the chemical and physical properties of the egg components (Min et al., 2005). Llave et al. (2018) confirmed the strong influence of temperature on the color changes of liquid egg samples due to thermal protein denaturation. For these reasons, as a confirmation of the expected color changes of the liquid egg samples processed of both approaches, CVS was used to compare the color values after each process versus the initial values, and the results are shown in **Table 3-3**.

No significant difference ($p \geq 0.05$) was observed between the raw liquid egg samples used in both approaches. The ΔE^* values of all liquid egg samples were small ($\Delta E^* < 3$), which is relevant since it has been reported that in this small range, the color difference could not be detected by the naked eye (de Souza & Fernández, 2011), which could be proved by the images shown in **Fig. 3-6**. Alamprese et al. (2019) reported that the ΔE^* after 70 °C × 1 min and 67 °C × 4.5 min of OH processing (intermittent energy was supplied to maintain the temperature) were 3.3 and 3.4, respectively (assessed using a colorimeter). They also reported a ΔE^* value of 4.2 after the conventional pasteurization process (using a heat exchanger plate at 65.5 °C for 3 min).

Table 3-3. Color changes in the liquid egg samples after OH processing at 20 kHz and 50 V for both experimental approaches 1 and 2 (n = 3 each).

Egg samples	Approaches	ΔL^*	Δa^*	Δb^*	ΔC^*	ΔE^*
White	**1**	1.56 ± 1.85	-0.51 ±0.42	0.00 ± 0.00	0.31 ±0.42	1.90 ± 1.50
	2	2.01 ± 0.78	-0.31 ± 0.65	0.00 ± 0.00	0.44 ± 0.57	2.07 ± 0.88
Whole	**1**	0.00 ± 1.01	0.82 ± 0.18	-1.33 ± 0.28	1.57 ± 0.14	1.76 ±0.13
	2	-0.48 ± 0.33	1.28 ± 0.42	-0.61 ± 0.29	1.45 ± 0.25	1.55 ± 0.13
Yolk	**1**	-0.66 ± 2.28	-1.46 ± 0.08	-0.63 ± 2.42	2.30 ± 0.61	2.82 ± 1.03
	2	0.74 ± 1.33	-1.18 ± 0.20	0.94 ± 1.53	1.49 ± 0.02	1.65 ± 0.03

*Approach 1: Only OH process.; Approach 2: OH process plus thermal keeping stage.

By comparing the X values (shown in **Fig. 3-5**) with the color change values (**Table 3-3**) of the liquid egg samples, it can be recognized that a very small color change occurred because a slight thermal protein denaturation happened during the OH approaches, which was due to the effective control of the target final temperature. For example, immediately after the end of the OH process (approach 1) and after the OH process plus thermal keep step (approach 2, with a total heating time of 10 min), the X values were 0.99, 0.99, 0.99, and 0.87, 0.89, and 0.96 for egg white, whole egg, and egg yolk, respectively.

Higher processing temperatures and uncontrolled processes can cause the unfolding of proteins (protein denaturation), which can produce an intense coagulation, resulting in the opaque white appearance of egg whites (Mine et al., 1990) or in the vivid yellow color appearance of egg yolks, especially at temperatures below 90 °C (Llave et al. 2018). In the present study, these color changes were not observed in the evaluated approaches.

3.4 Conclusion

In this study, the temperature non-uniformity at of liquid egg samples occurred during OH pasteurization, although it is well known as a volumetric heating method that offers better temperature uniformity than traditional methods. This had a direct impact into accomplish pasteurization standards in delicate samples

such as liquid eggs. Temperature distribution of the whole materials during OH is hard to confirm by experimental measurement directly, and the computer simulation analysis is needed.

Although it can be observed that the center of egg white and yolk achieved the pasteurization standard (*P*-value above 10 min) after a short processing time, the *P*-values at the top corner remained at approximately 0 because the temperature it reached was not high enough. In the case of whole eggs, the pasteurization standard was not reached even at the center.

The liquid egg samples kept high quality (*X* values kept high and the color had nearly no change) after 10 min processing (including OH and thermal keep approaches), but considering that the pasteurization effect had not fully achieved the standards, the heating conditions needed to be further considered and optimized.

3.5 References

Alamprese, C., Cigarini, M., & Brutti, A. (2019). Effects of ohmic heating on technological properties of whole egg. *Innovative Food Science and Emerging Technologies*, 58, 102244.

Cappato, L. P., Ferreira, M. V., Guimaraes, J. T., Portela, J. B., Costa, A. L., Freitas, M. Q., et al. (2017). Ohmic heating in dairy processing: Relevant aspects for safety and quality. *Trends in Food Science & Technology*, 62, 104–112.

de Souza, P. M., & Fernández, A. (2011). Effects of UV-C on physicochemical quality attributes and *Salmonella enteritidis* inactivation in liquid egg products. *Food Control*, 22(8), 1385–1392.

Darvishi, H., Khoshtaghaza, M. H., Zarein, M., & Azadbakht, M. (2012). Ohmic processing of liquid whole egg, white egg and yolk. Agricultural Engineering International: *CIGR Journal*, 14(4), 224-230.

EFSA & ECDC, European Food Safety Authority & European Centre for Disease Prevention and Control (2011). The European Union summary report on trends and sources of zoonoses, zoonotic agents and food-borne outbreaks in 2009. *EFSA Journal*, 9(3), 2090, 378 pp.

Garibaldi, J. A., Straka, R. P., & Ijichi, K. (1969). Heat resistance of Salmonella in various egg products. *Applied Microbiology*, 17(4), 491–496.

Goullieux, A., & Pain, J.-P. (2005). Ohmic heating. In Emerging technologies for food processing (pp. 469-505).

IEC 61966-2-1, 1999. Multimedia systems and equipment – Colour measurements and management – Part 2-1: Colour management – Default RGB color space – sRGB' (International Electrotechnical Commission, Geneva, 1999-10).

Jaeger, H., Roth, A., Toepfl, S., Holzhauser, T., Engel, K. H., Knorr, D., et al. (2016). Opinion on the use of ohmic heating for the treatment of foods. *Trends in Food Science & Technology*, 55, 84–97.

Jun, S., & Sastry, S. (2007). Reusable pouch development for long term space missions: A 3D ohmic model for verification of sterilization efficacy. *Journal of Food Engineering*, 80(4), 1199–1205.

Knirsch, M. C., Dos Santos, C. A., Vicente, A., & Penna, T. C. V. (2010). Ohmic heating–a review. *Trends in Food Science & Technology*, 21(9), 436–441.

Koç, M., Koç, B., Susyal, G., Yilmazer, M. S., Ertekin, F. K., & Bağdatlıoğlu, N. (2011). Functional and physicochemical properties of whole egg powder: effect of spray drying conditions. *Journal of Food Science and Technology*, 48(2), 141–149.

Laca, A., Paredes, B., & Díaz, M. (2010). A method of egg yolk fractionation. Characterization of fractions. Food Hydrocolloids, 24(4), 434-443.

Li-Chan, E. C., & Kim, H. O. (2008). Structure and chemical composition of eggs. Egg bioscience and biotechnology, 10, 9780470181249.

Llave, Y., Shibata-Ishiwatari, N., Watanabe, M., Fukuoka, M., Hamada-Sato, N., & Sakai, N. (2017a). Analysis of the effects of thermal protein denaturation on the quality attributes of sous-vide cooked tuna. *Journal of Food Processing and Preservation*, 42(1), e13347.

Llave, Y., Takemori, K., Fukuoka, M., Takemori, T., Tomita, H., & Sakai, N. (2017b). Analysis of browning of broiled foods by noncontact techniques: A case study for Japanese eggplant (*Solanum melongena*). *Journal of Food Process Engineering*, 40(1), e12347.

Llave, Y., Fukuda, S., Fukuoka, M., Shibata-Ishiwatari, N., & Sakai, N. (2018). Analysis of color changes in chicken egg yolks and whites based on degree of thermal protein denaturation during ohmic heating and water bath treatment. *Journal of Food Engineering*, 222, 151–161.

Marra, F., Zell, M., Lyng, J. G., Morgan, D. J., & Cronin, D. A. (2009). Analysis of heat transfer during ohmic processing of a solid food. *Journal of Food Engineering*, 91(1), 56–63.

Mendoza, F., Dejmek, P., & Aguilera, J. M. (2006). Calibrated color measurements of agricultural foods using image analysis. *Postharvest Biology and Technology*, 41(3), 285–295.

Mine, Y., Noutomi, T., & Haga, N. (1990). Thermally induced changes in egg white proteins. *Journal of Agricultural and Food Chemistry*, 38(12), 2122–2125.

Min, B. R., Nam, K. C., Lee, E. J., Ko, G. Y., Trampel, D. W., & Ahn, D. U. (2005). Effect of irradiating shell eggs on quality attributes and functional properties of yolk and white. *Poultry Science*, 84(11), 1791–1796.

Monfort, S., Mañas, P., Condón, S., Raso, J., & Álvarez, I. (2012). Physicochemical and functional properties of liquid whole egg treated by the application of pulsed electric fields followed by heat in the presence of triethyl citrate. *Food Research International*, 48(2), 484–490.

Mukhopadhyay, S., & Ramaswamy, R. (2012). Application of emerging technologies to control Salmonella in foods: A review. *Food Research International*, 45(2), 666–677.

Nakai, T., Kami, N., Fukuoka, M., & Sakai, N. (2018). Ohmic heating behavior of whole egg and measurement of electrical conductivity of egg constituents. Japan Journal of Food Engineering, 19(4), 199–207 (in Japanese).

Rec. ITU-R BT.709-5, 2002. Parameter values for the HDTV standards for production and international programme exchange (1990, revised 2002). International Telecommunication Union, 1211 Geneva 20, Switzerland.

Su, H. P., & Lin, C. W. (1993). A new process for preparing transparent alkalised duck egg and its quality. Journal of the Science of Food and Agriculture, 61(1), 117-120.

Sánchez-Gimeno, A. C., Vercet, A., & López-Buesa, P. (2006). Studies of ovalbumin gelation in the presence of carrageenans and after manothermosonication treatments. *Innovative Food Science and Emerging Technologies*, 7(4), 270–274.

Takano Mitsuo & Yokoyama Michio (1998). *Inactivation of Food-borne Microorganism* (in Japanese), first version, Saiwai Shobo, pp. 127-13.

Villota, R., & Hawkes, J. G. (2007). Reaction kinetics in food systems. In: Heldman, D.R., Lund, D.B. (Eds.), Handbook of Food Engineering, second ed. CRC Press, New York, pp. 125–286.

CDC, Centers for Disease Control and Prevention Salmonella infections linked to Gravel ridge farms shell eggs (2018). https://www.cdc.gov/salmonella/enteritidis-09-18/index.html. Accessed May 28, 2021.

MHLW, Ministry of Health, Labour and Welfare (1959). Standards for each food, bird egg. https://www.mhlw.go.jp/file/06-Seisakujouhou-11130500-Shokuhinanzenbu/0000094499.pdf. Accessed May 28, 2021

Chapter 4 – Computer simulation and ohmic heating conditions optimization for liquid egg samples

4.1 Introduction

As a novel heating method, OH has certain advantages, such as uniform and rapid heating, higher energy efficiency, and fouling reduction (Mercali et al., 2014). Products processed via OH tend to have a better quality, including structural integrity, flavor, and nutrient retention, compared with those processed using conventional heating (Seyhun et al., 2013). Unfortunately, non-uniform temperature distribution during OH has also been reported (Cappato et al., 2017).

Plenty of research has been carried out to study about OH of food products on various aspects, among which temperature distribution is a critical factor to be discussed when better quality of food product is required.

The temperature distribution and the location of "cold spots" and "hot spots", which highly influence the quality deterioration and safety of food products, respectively, during the OH process need to be considered especially since its effects cannot be extrapolated from the current knowledge of conventional heating (Knirsch et al., 2010). Therefore, the assessment of uniform temperature distributions during OH processes is particularly important, and computer simulation is needed.

Marra, et al. (2009) pointed out that when applying OH on food products, mathematical models of the progressing, as an invaluable aid for understanding and validation of thermal technologies, should be developed to identify possible hot and cold spots, in order to quantify heat losses and to evaluate the influence caused by main factors on the product during the thermal progress, thus ensure completely safe of products treated by OH. Many computer simulation models for OH simulation have been published in the past years (Engchuan, et al., 2014; Guo, et al., 2017; Jun & Sastry, 2007; Marra et al., 2009; Tumpanuvatr & Jittanit, 2012). As an example, the temperature distribution including cold spots of materials (mashed potato), which had uniform electrical conductivity (EC), had been successfully predicted using computer simulation by Marra et al. (2009).

In this Chapter, a 3-D computer simulation model for OH at high frequencies of liquid egg samples was established and calculated by the finite element method (*FEM*) using COMSOL Multiphysics 5.6 software. The experimental temperature profiles of liquid egg samples at different locations recorded during OH and thermal keep approaches have been recorded in **Chapter 3**, which were used in this chapter for the comparison with the simulated results. After the simulation models were accurately validated, the

pasteurization effect (*P*-value) and thermal protein non-denaturation ratio (*X*) were calculated and simulated based on the temperature profiles. Then the processing conditions were optimized by computer simulation.

The specific aims of this chapter were to:

1. verify the accuracy of the simulation models via comparing the experimental and simulated results;
2. identify the hot and cold spots of liquid egg white, yolk, and whole egg during OH processing by analyzing the temperature distribution via computer simulation;
3. evaluate the pasteurization effect (*P*-value) against *Salmonella typhimurium* and the thermal protein non-denaturation ratio (*X*) of liquid egg samples during OH processing by numerical simulation; and
4. optimize the heating conditions to ensure that the liquid egg samples achieved the required degree of pasteurization while retaining quality attributes [combined thermal protein denaturation with color (showed in **Chapter 3**)].

4.2 Materials and Methods

4.2.1 Computer simulation development

A 3-D computer simulation model was established and calculated by the finite element method (*FEM*) using COMSOL Multiphysics 5.6 software, and the details of model establishment are shown as following:

(1) Geometry and materials setting

A 3-D model (Model 1) was established of which the size and materials were based on experimental conditions, as **Fig. 4-1** showing.

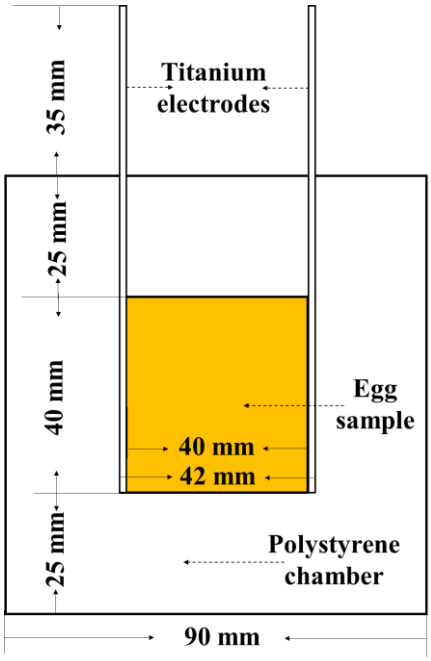

Fig. 4-1 Schematic diagram of the central vertical cross-section of the geometry and material settings of Model 1 for simulated approaches 1 and 2.

The following simulated approaches (1 and 2) also followed the experimental conditions:

Approach 1: OH process only, as shown in experimental approach 1 in **Fig. 4-2.**

Approach 2: OH process and thermal keep approach, as experimental approach 2 in **Fig. 4-2**. The liquid egg samples were held in a polystyrene (thermal insulation) chamber and heated via OH (50 V, 20 kHz) from 20 °C to target temperature of liquid egg samples during heating (*Tt*, 59.1 ℃ for egg white and whole egg and 63.3 ℃ for egg yolk) (step 1), after which OH was stopped and the samples were held inside the polystyrene chamber to complete pasteurization using the residual temperature (step 2).

The simulation flow steps are shown in **Fig. 4-2**.

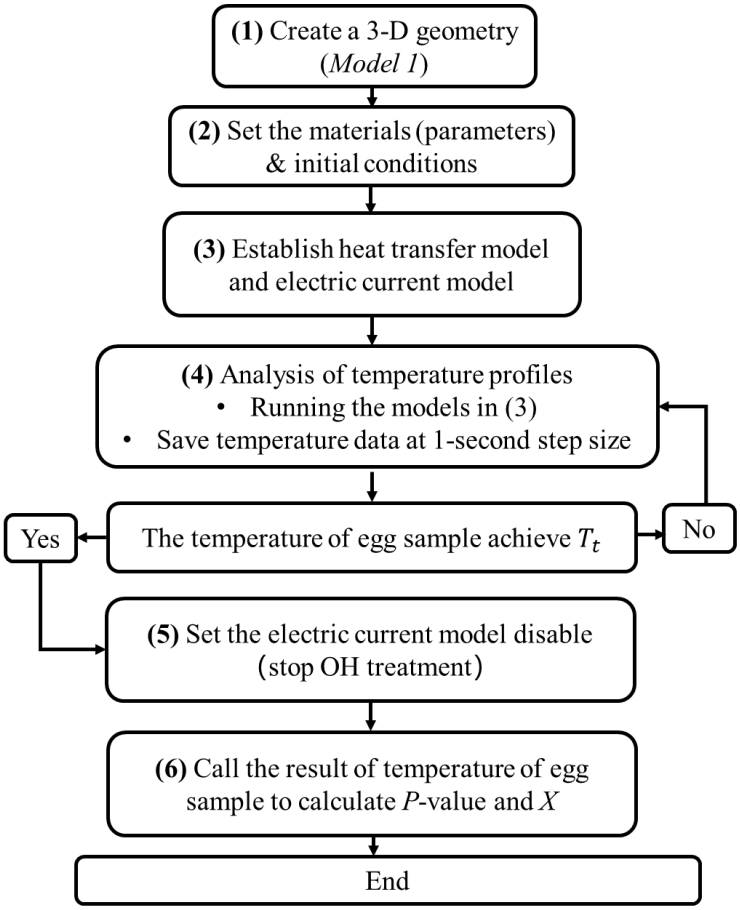

Fig. 4-2 Schematic diagram of the simulation flow of Model 1.

The parameters of the materials used in the simulation are listed in **Table 4-1**. The thermophysical properties of the liquid egg samples were obtained from Coimbra et al. (2006). The water content mass fraction (*Ww*) was 0.884, 0.482, and 0.761 for egg white, egg yolk, and whole egg, respectively, according to the standard tables of food composition in Japan (MEXT, 2015). The EC of the samples, σ (S·m-1), was calculated as explained in **Chapter 2**.

Table.4-1 Values of the properties of the samples and materials used in simulation.

Material	ρ [kg m^{-3}][1, 2, *]	C_p [J·g^{-1} K^{-1}][1, 2, *]	k [W m^{-1} K^{-1}][1, 2, *]	σ [S m^{-1}] **
Egg white	1295.72-0.0559T	0.668+0.0025T	0.276-0.0004T	0.0172T
	-284.43W_w	+2.4429W_w	+0.4302W_w	-4.3032
Egg yolk	1295.72-0.0559T	0.668+0.0025T	0.276-0.0004T	0.0064T
	-284.43W_w	+2.4429W_w	+0.4302W_w	-1.6066
Whole egg	1295.72-0.0559T	0.668+0.0025T	0.276-0.0004T	0.0113T
	-284.43W_w	+2.4429W_w	+0.4302W_w	-2.8351
Acrylic	1190	1.47	0.18	0
Titanium	4510	0.52	17	17.36×10^{5}
Polystyrene	32.84	1.50	0.028	0
Air	-	$10^{-3}\times$ (1047.63657 -0.372589265×T +9.45304214×$10^{-4}\times T^2$ -6.02409443×$10^{-7}\times T^3$ +1.2858961×$10^{-10}\times T^4$)	-0.00227583562 +1.15480022×$10^{-4}\times T$ -7.90252856×$10^{-8}\times T^2$ +4.11702505×$10^{-11}\times T^3$ -7.43864331×$10^{-15}\times T^4$	-

[1]T is the absolute temperature [K]

[2]W_w is the water content in mass fraction of egg materials (MEXT, 2015).

*The thermal-physical properties (ρ, C_p and k) of liquid egg samples were obtained from Coimbra et al., (2006).

**The electrical conductivity (σ) of liquid egg samples were measured in this study (Fig. 2B).

***C_p, k, and μ equations of air were obtained from the material library of COMSOL (2021b). For the dynamic viscosity of air (μ, Pa s) was used:

0.6×(-8.38278×10^{-7}+8.35717342×10^{-8}×T-7.69429583×10^{-11}×T^2+4.6437266×10^{-14}×T^3-1.06585607×10^{-17}×T^4

(2) Governing equations, boundary conditions, and solution procedures

(2-1) Electric current: Electric potentials of 50 V and 0 V were set as the two boundaries of each titanium

electrode. Domain current conservation was set to all domains during OH (COMSOL, 2020a).

$$\nabla \cdot \mathrm{J} = \mathrm{I_{j,v}} \quad (1)$$

$$\mathrm{J} = \sigma \mathrm{E} + \frac{\partial \mathrm{D}}{\partial \mathrm{t}} + \mathrm{J_e} \quad (2)$$

$$\mathrm{E} = -\nabla V \quad (3)$$

where J is the current density ($A \cdot m^{-3}$), $I_{j,v}$ is the volumetric source of the current ($A \cdot m^{-3}$), σ is the EC ($S \cdot m^{-1}$), J_e is the externally generated current density ($A \cdot m^{-2}$), D is the electric displacement ($C \cdot m^{-2}$), V is the electric potential (V), and E is the electric field (V).

(2-2) Heat transfer in solids: In the analysis of heat transfer, stationary liquids (like the liquid egg samples in this study) could be regarded as solids, which saves computing resources and has almost no effect on the simulation results (COMSOL, 2021a). Heat transfer in solids was applied to all domains (liquid egg samples were also set as solids during the simulation because they did not show flow during the OH process).

The initial temperature of all domains and the environmental temperature were set at 20 °C. The governing equations for heat transfer are as follows:

$$\rho C_P \frac{\partial T}{\partial t} + \rho C_P u \cdot \nabla T + \nabla \cdot q = Q \quad (4)$$

$$q = -k \nabla T \quad (5)$$

where ρ is the density of the materials ($kg \cdot m^{-3}$), C_p is the specific heat capacity ($J \cdot kg^{-1}\ K^{-1}$), T is the temperature (K), u is the air velocity field ($m \cdot s^{-1}$), Q is the heat source ($W \cdot m^{-3}$), k is the thermal conductivity ($W \cdot m^{-1}\ K^{-1}$), and q is the conductive heat flux ($W \cdot m^{-2}$).

For simulated approaches 1 and 2 using model 1 (**Fig. 4-3**), boundary 1 was set as thermally insulated at the bottom because it was connected to the test bench during the OH process (COMSOL, 2021a); thus, it was considered to be at a constant room temperature. Boundary 2 (vertical boundary of the model) and boundary 3 (horizontal boundary of the model) of model 1 were set as external natural convection vertical walls (Eqs. 6 and 7) and the upside horizontal plate (Eqs. 6 and 8), respectively (COMSOL, 2020b & 2021a).

$$q = h(T_{amb} - T) \quad (6)$$

$$h = \frac{k_a}{L}\left(0.825 + \frac{0.387 Ra_L^{1/6}}{\left(1+\left(\frac{0.492 k_a}{\mu_a C_{p,a}}\right)^{9/16}\right)^{8/27}}\right)^2 \quad (7)$$

$$h = \frac{k}{L} 0.27 Ra_L^{1/4} \quad (8)$$

where q is the conductive heat flux ($W \cdot m^{-2}$), h is the heat transfer coefficient ($W \cdot m^{-2}\ K^{-1}$), T_{amb} is the ambient temperature (°C), L is the length of each model (m), k_a is the thermal conductivity of air ($W \cdot m^{-1}\ K^{-1}$), μ_a is the dynamic viscosity of air (Pa·s), $C_{p,a}$ is the heat capacity of air at constant pressure ($J \cdot kg^{-1}\ K^{-1}$), and Ra_L is the Rayleigh number.

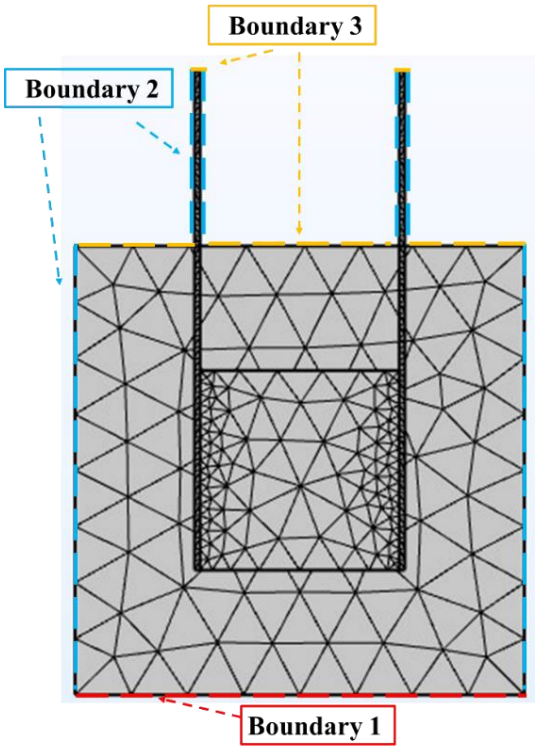

Fig. 4-3 Schematic diagrams of the central vertical cross-section of mesh and boundary settings of model 1 for simulated approaches 1 and 2.

(2-3) Protein denaturation modeling: The chemistry and transport of diluted species module in COMSOL simulation was applied to the domains of the egg sample. We set the diluted species *before* and *after* the OH process as the non-denatured protein and denatured protein, respectively (the limit values of *before* and *after* were set to 0.9999 and 0.0001, respectively). Moreover, an irreversible reaction was set, the reaction rate was set as automatic, and the reaction rate constant was assumed to follow the Arrhenius equation (Eq. 9).

$$k_{ti} = Z_i\ exp\left(-\frac{E_{ai}}{R_t T}\right) \qquad i = 1,2 \tag{9}$$

where Z_i is the pre-exponential factor (min^{-1}), E_{ai} is the activation energy of denaturation ($kJ \cdot mol^{-1}$), R_t is the gas constant ($J \cdot K^{-1} mol^{-1}$), and T is the absolute temperature (K). The Z_i and E_{ai} values were reported

in a previous study (Llave et al., 2018), as **Table 4-2** showing:

Table.4-2 Kinetics parameters [activation energy (E_{ai}) and pre-exponential factor (Z_i)] of the thermal protein denaturation of liquid egg white and egg yolk.

	E_{ai} (kJ·mol^{-1})	Z_i (min^{-1})
Ovalbumin of egg white	202.3 ± 1.7	$1.61 \times 10^{30} \pm 0.001$
Low-density lipoproteins of egg yolk	600.3 ± 2.5	$1.83 \times 10^{91} \pm 0.004$

Simulated results of temperature profiles of the domain of liquid egg samples during approaches 1 and 2 calculated in section 4.2.1 (2-2) were called to calculate the thermal protein denaturation reaction using Eq. (9). And the protein non-denaturation ratio (X) was defined as the ratio of the concentrations of non-denatured protein (the diluted species *before*) at the initial state (C_{i0}, set as 0.9999) to that at time t (C_{it}). It was directly expressed as C_{it} because C_{i0} is close to 1.

(2-4) Pasteurization value modeling: The domain integration module was used to permit the temperature results of the egg sample domain to be called for calculating the P-value within per unit time step (the time step was 1 s in this study) using Eq. (10).

$$P' = t \times 10^{\frac{T - T_{ref}}{Z_t}} \qquad (10)$$

where P' is the P-value in per unit time step (min), t is the unit time for heating (min), T is the temperature of the sample called from 4.2.1 (2-2) (°C), T_{ref} is the standard temperature of liquid eggs for pasteurization (°C), and Z_{t} is the slope of the thermal destruction-time curve (°C) for a standard reference strain of *Salmonella typhimurium*. The T_{ref} values were selected based on the standard values defined by the Japanese Ministry of Health, Labor, and Welfare as 54 °C, 58 °C, and 59 °C for egg white, whole egg, and egg yolk, respectively (MHLW, 1959). The Z_{t} values used in Eq. (2) were 4.2 °C, 4.3 °C, and 4.4 °C for liquid egg white, whole egg, and egg yolk, respectively (Garibaldi et al., 1969).

Then the P-value profiles and distributions were obtained after integration using Eq. (11) in domain integration module.

$$P = \int P' dt \qquad (11)$$

where P is the P-value during processing (min), P' is the P-value in per unit time step (min), t is the heating time (min).

(3) Mesh generation

Normal size and physics-controlled free tetrahedral meshes were generated for the entire setup geometry. The numbers of tetrahedrons and average element qualities were generated depending on the size and materials of each geometry for Model (**Fig. 4-3**), and the details of the mesh settings are shown in **Table 4-3**. The geometry and materials of model 1 (for simulated approaches 1 and 2) were created according to the experimental conditions. For simulated approach 2, heat transfer and electric current were run to simulate the OH step, then the electric current was set as disabled (heat transfer kept running) to simulate the thermal keep approach when the temperature of the liquid egg sample achieved (Tt, to obtain the temperature results). The temperature results were then used to calculate the P-value and X values.

Table.4-3 Mesh settings (numbers of tetrahedrons and average element qualities) in each domain of simulation Model 1.

	Electrodes	**Polystyrene**	**Egg sample**
Number of tetrahedrons	4113	7776	2302
Average element quality	0.4422	0.6504	0.6533

- The average element quality is a method to inspect the quality of the mesh developed in COMSOL Multiphysics (COMSOL, 2017). A quality of 1 is the best possible and it indicates an optimal element, while 0 represents a degenerated element. Elements with a quality above 0.1 are considered to be of good quality for many applications.

4.2.2 Optimization of OH pasteurization by computer simulation

The cold zone would occur at the surfaces of liquid egg samples because of the thermal loss to the chamber and electrodes during OH processing as **Chapter 3** shown, which leaded to the nonuniformity of temperature distribution and had negative effect for pasteurization. For these reasons，the OH pasteurization

conditions need to be optimized, and the Model 2 was established to solve the problems.

The parameters used in Model 2 were same as Model 1, as **Table 4-1** shown. The details of optimization are shown as follows:

(1) Geometry and materials setting

The optimized 3-D model (Model 2) was established for pasteurization conditions optimization as **Fig. 4-4** showing.

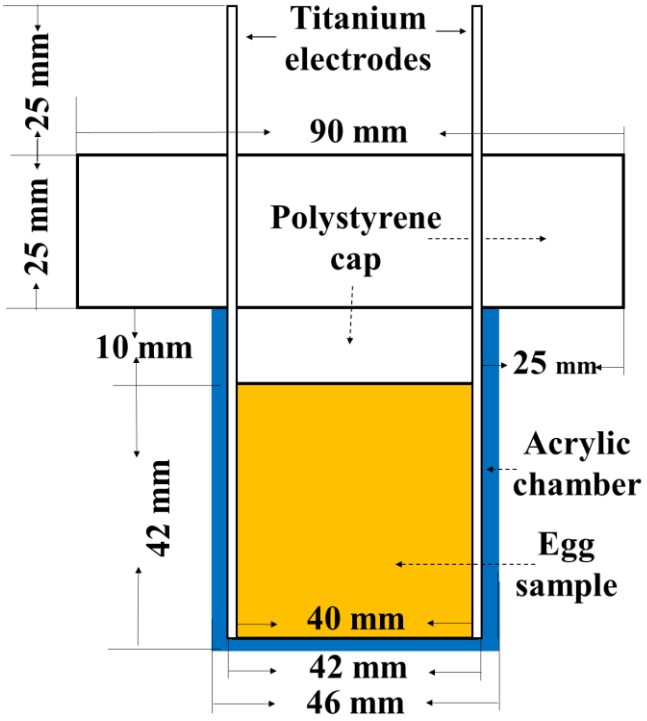

Fig. 4-4 Schematic diagram of the central vertical cross-section of the geometry and material settings of Model 2 for simulated approaches 3 and 4.

The simulation flow steps of Model 2 are shown in **Fig. 4-5**. And the detail information of the simulated approaches used for the optimization of the OH pasteurization is explained as follows:

Approach 3: OH process plus an external heating approach, which started after the OH process ended (**Fig.4-6**). The liquid egg samples were held in an acrylic chamber covered with a polystyrene layer (thermal insulation) and heated via OH (50 V, 20 kHz) from 20 °C to T_t (step 1), which was then changed into an external heating system (heating temperature kept at T_t, step 2).

Approach 4: OH plus concurrent external heating approach (**Fig.4-6**). The liquid egg samples were held in an acrylic chamber covered with a concurrent external heating system and heated via OH (50 V, 20 kHz), where the temperature of the external heating system was set 1 °C higher than the center temperature of the egg sample (to avoid temperature drop due to heat loss when heat passes through the acrylic container wall) from 20 °C to T_t (step 1). After reaching T_t, OH was stopped, and the external heating temperature was set to maintain the T_t (step 2).

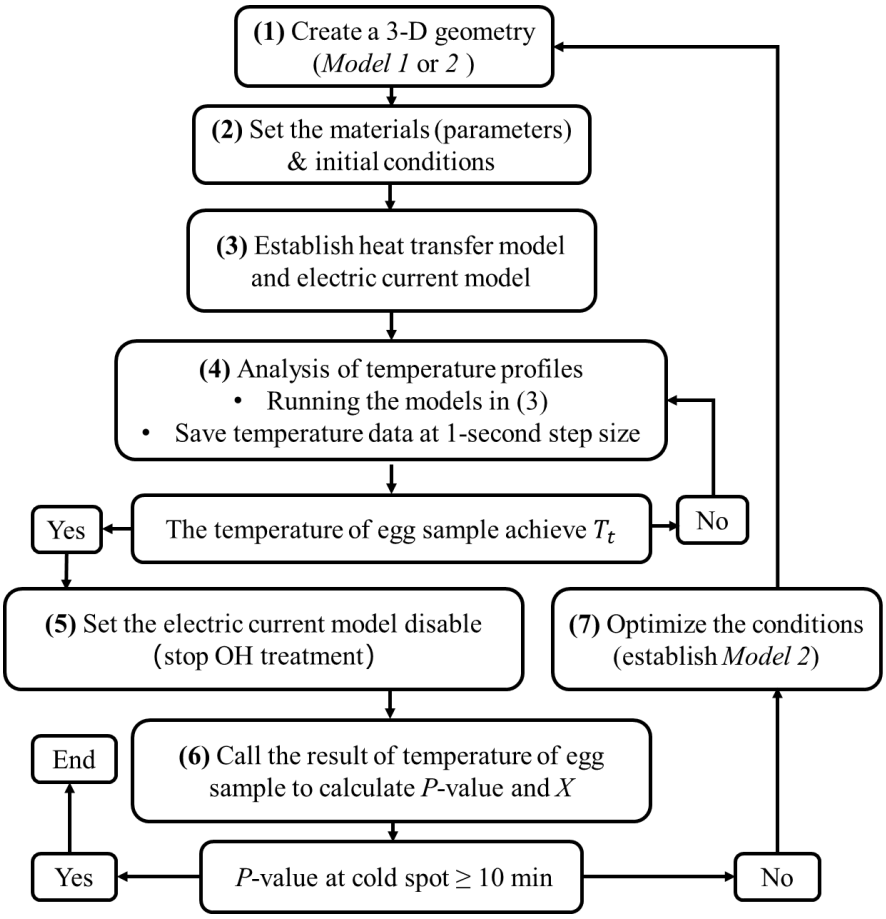

Fig. 4-5 Schematic diagram of the simulation flow of Model 2.

(2) Governing equations, boundary conditions, and solution procedures

(2-1) Electric current: the settings are same as Model 1 in Section **4.2.1.**

(2-2) Heat transfer in solids:

For simulated approach 3 using model 2 (**Fig. 4-6**), boundary 1 was set as thermally insulated during OH. After the OH process was stopped, boundary 1 was set at a constant temperature (T_t). Boundaries 2 and 3

were set as an external natural convection and as a thermal insulator after the OH process (similar to approaches 1 and 2 using model 1), respectively.

For simulated approach 4 using model 2 (**Fig. 4-6**), boundary 1 was set as a concurrent external heating system, as described in section 2.8.1, and the temperature was calculated using Eq. 12. The conditions of the other boundaries were set as for simulated approach 3. The external natural convection of the vertical wall and the upside horizontal plate were calculated using Eqs. 6 and 7, and Eqs. 6 and 8, respectively.

$$T_{ext} = \frac{T_t - T_1}{t_0} \times t + T_2 \qquad (12)$$

where T_{ext} is the temperature of the external heating system during processing, T_t is the target temperature of liquid egg samples during heating (59.1 °C for egg white and whole egg and 63.3 °C for egg yolk), T_1 is the temperature of the liquid egg samples (initially 20 °C for each sample), T_2 is the initial temperature of the external heating system set at 1 °C higher than the initial temperature of the egg sample (21 °C), t is the OH time (s), and t_0 is the total heating time of the liquid egg samples until T_t was achieved (89 s, 130 s, and 214 s for egg white, whole egg, and egg yolk, respectively).

The other settings are same as Model 1 in Section **4.2.1.**

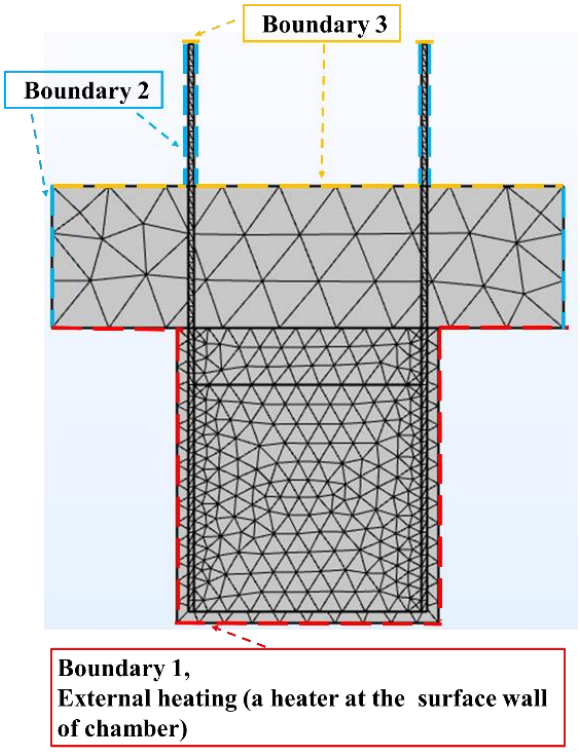

Fig. 4-6 Schematic diagrams of the central vertical cross-section of mesh and boundary settings of model 2 for simulated approaches 3 and 4.

(2-3) Protein denaturation modeling: the settings are same as Model 1 in Section **4.2.1.**

(2-4) Pasteurization value modeling: the settings are same as Model 1 in Section **4.2.1.**

(3) Mesh generation

Normal size and physics-controlled free tetrahedral meshes were generated for the entire setup geometry. The numbers of tetrahedrons and average element qualities were generated depending on the size and materials of each geometry for Model (**Fig. 4-6**), and the details of the mesh settings are shown in **Table 4-4**.

Table.4-4 Mesh settings (numbers of tetrahedrons and average element qualities) in each domain of simulation Model 2.

	Electrodes	**Polystyrene**	**Egg sample**
Number of tetrahedrons	5273	5170	3254
Average element quality	0.4479	0.6474	0.6545

- The average element quality is a method to inspect the quality of the mesh developed in COMSOL Multiphysics (COMSOL, 2017), as same as **Table 4-3**.

4.2.3 Solution strategy

The Model 1 was established depending on the experimental conditions as **Chapter 3** shown, to do the comparation of experimental and simulated results and verify the accuracy of the computer simulation analysis. The details of simulation flow are shown as following:

(1) the 3D geometric were established by COMSOL Multiphysics 5.6 software;

(2) the parameters of each materials (as **Table 4-1** showing) were set to corresponding parts of the model;

(3) the electricity field (using Eqs. 1-3) and thermodynamic field (using Eqs. 6-8) were added to corresponding parts of the model and combined (using Eqs. 4 and 5) to obtain the temperature profiles

via simulating the OH and thermal keep approaches using finite element method (as section 2-1 and 2-2 showing);

(4) the results of temperature profiles were called to calculate the protein non-denaturation ratio (*X*) and *P*-value

The simulated results of temperature profiles, *P*-value, and *X* were obtained and compared with experimental results, from which we could know that it is hard to achieve the pasteurization standard for liquid egg samples at surface parts under these conditions. And the Model 2 for processing conditions optimization was established by adding an external heating system because the modeling accuracy had been proved. Then, the simulation flow was repeated as Model 1, and the results were obtained. And It was proved that OH combined with a concurrent external heating approach was successful in reducing non-uniformities in temperature, which could accomplish the pasteurization standards for liquid egg samples while avoiding excessive thermal protein denaturation caused by local overheating.

4.3 Results and Discussion

4.3.1 Temperature, pasteurization value, and *X* evaluation of egg samples of Model 1

(1) temperature evaluation of egg samples during OH and thermal keep approaches

The temperature profiles at the center and the top corner of the liquid egg samples during OH and OH plus thermal keep approach (simulated approaches 1 and 2, respectively) were compared to the experimentally measured values (experimental approaches 1 and 2) in **Fig. 4-7**.

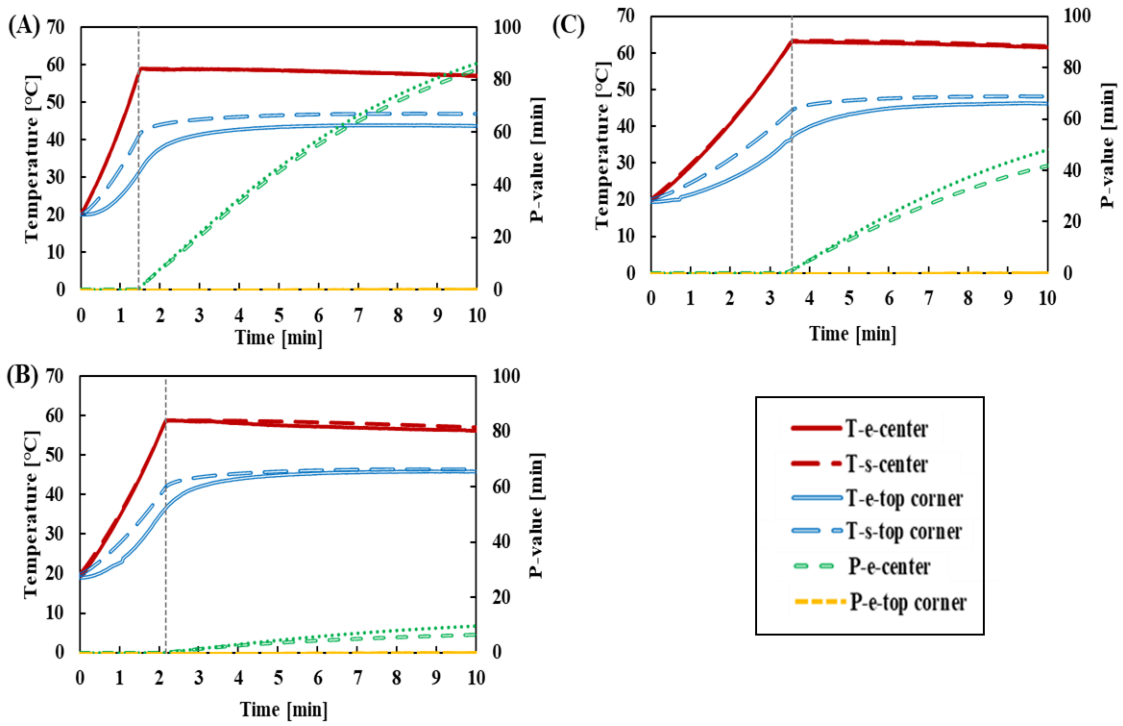

Fig. 4-7 Comparison of the temperature and *P*-value profiles of egg white (A), whole egg (B), and egg yolk (C) samples during OH (20 kHz and 50 V) plus thermal keeping stage (experimental and simulated approaches 1 and 2). T: temperature, P: *P*-value, e: experimental result, s: simulated result.

It was observed that the simulated results of the temperature at the center were closer to the experimental results; whereas at the top corner, a slight temperature difference was observed because a small amount of air might have entered the top of the sample chamber during the experiments, resulting in a slight heat loss. A similar phenomenon was observed in the study of Marra et al. (2009), form which the heat losses to the electrodes and chamber surfaces had been pointed out as the key factor leaded to the temperature difference at different locations of EC uniformity materials. And these heat losses in the chamber surfaces (in contact with the sample) and electrodes have been reported to be critical for sterilization (including pasteurization) calculations (Jun & Sastry, 2007).

Computer simulation has been used for OH processing analysis and here are some examples at high frequencies: Guo et al. (2017) reported the study of OH at 50 Hz and 20 kHz for two-component foods (consisting of mashed potato and mashed potato with 1% NaCl) configured using four different filling patterns (parallel, series, and two concentric patterns), including experiment and computer simulation, which is considered would assist in the design of food sterilization and pasteurization processes and

contribute in industrial applications for a better design of OH systems and electrode configurations for rapid and uniform heating. Jin et al. (2020) obtained the accurate temperature distribution of yellowtail (*Seriola quinqueradiata*) fillets during OH at 20 kHz via computer simulation.

Anyway, the simulated results were close to the experimental results, which could provide that the models for simulation were credible and accurate. And the simulated temperature distributions of the three egg samples at the end of each of the simulated approaches 1 and 2 are shown in **Fig. 4-8**. In general, for the simulated approaches, the center part coincided with the hottest spot, and the positions near the external top surface coincided with the coldest spot. The external top surface position of the system showed thermal losses, owing to the contact between the sample and chamber. This could be because the top part of the electrodes was exposed to air during its connection to the heating machine; thus, the samples slightly lost heat to the air along the tangential direction, which caused a drop in the temperature of the top corner for all liquid egg samples.

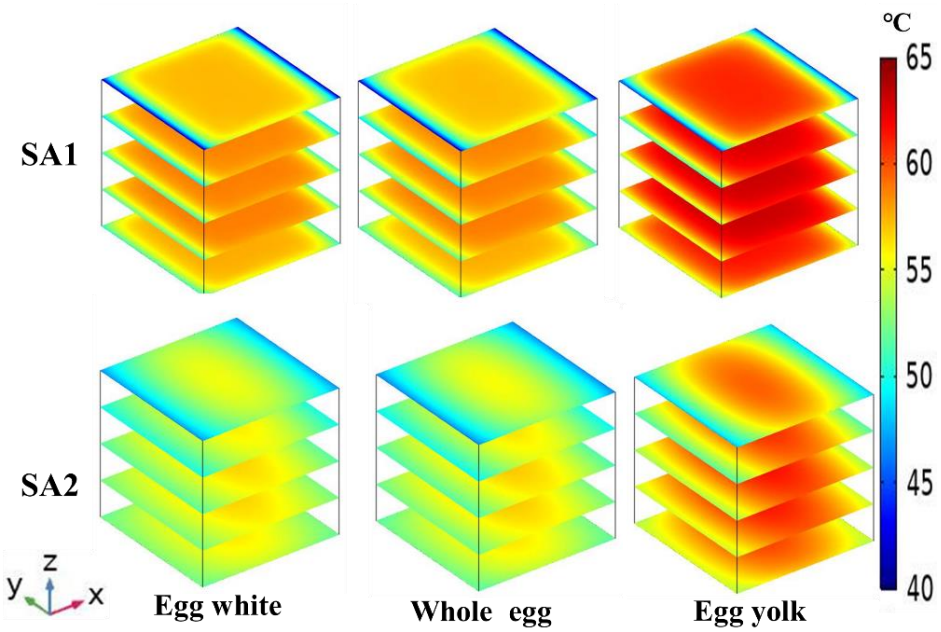

Fig. 4-8 Temperature distribution in the horizontal cross sections of liquid egg samples during the OH process (20 kHz and 50 V) (simulated approach 1 – SA1, at the end of OH [89, 130, and 214 s for egg white, whole egg, and yolk, respectively]; simulated approach 2 – SA2, at the end of OH and thermal keep processing (the total processing time was 10 min). Egg samples were connected to the electrodes in the X-axis direction.

(2) Pasteurization effect evaluation

The pasteurization effect was evaluated using the *P*-value calculated in Eq. (10). Moreover, it was verified that the accomplishment of the Japanese normative (MHLW, 1959) was more than 10 minutes for liquid egg samples.

The *P*-value profiles at the center (T_h) and top corner (T_c) of the three liquid egg samples during OH and the thermal keep approach are shown in **Fig. 4-7** (experimental and simulated approaches 1 and 2, conducted with model 1). Although it can be observed that the center of egg white and yolk achieved the pasteurization standard (*P*-value above 10 min) after a short processing time, the *P*-values at the top corner remained at approximately 0 because the temperature it reached was not high enough. In the case of whole eggs, the pasteurization standard was not reached even at the center (T_h).

The *P*-value distributions under simulated approaches 2 at several vertical cross-sections and time intervals are shown in **Fig. 4-9.** For simulated approach 2 (**Fig. 4-9**), after 10 min (including 89, 130, and 214 s of OH for egg white, whole egg, and egg yolk, respectively), only the center part of the egg whites achieved the pasteurization standard. However, the required pasteurization degree of the entire sample was not attained even after 20 min of processing for any of the samples. At this time, although the center parts of the three setups showed *P*-values above 10 min, in other parts, the *P*-value standard was not reached or it was extremely high at the center (evidence of overheating) for whole egg and egg white.

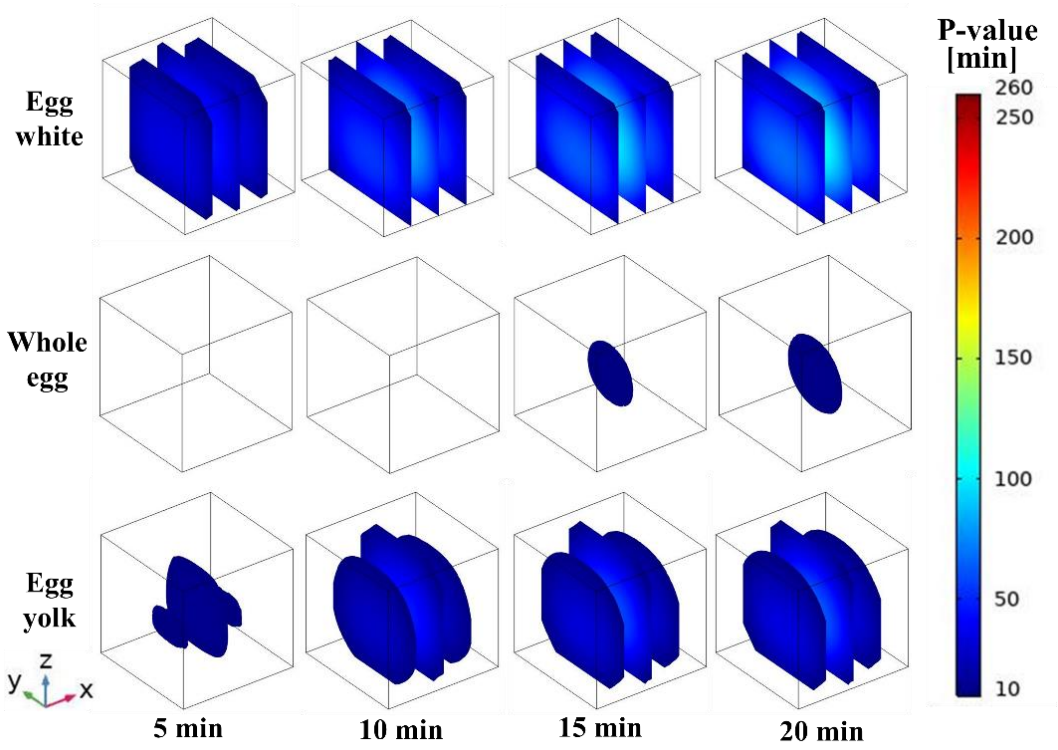

Fig. 4-9 Simulated P-value distributions (for P-values ≥ 10) at several vertical cross sections of liquid egg samples and time intervals during the OH treatment process at 20 kHz and 50 V, under simulated approaches 2. Liquid egg samples were connected to the electrodes in the X-axis direction.

(3) Protein denaturation evaluation

The ovalbumin and low-density lipoproteins (LDL) began denaturing at 59.17 ℃ and 63.33 ℃ for egg white and egg yolk, respectively (Llave et al., 2018). For the whole egg samples, the denaturation degree was focused on ovalbumin (as in the case of egg white) because the temperature during the process (58 °C) did not reach the protein denaturation temperature of LDL.

As shown in **Fig. 4-10**, the degree of protein denaturation of liquid egg samples was evaluated using the protein non-denaturation ratio (X) under experimental and simulated approaches 2, From the results, it can be concluded that egg yolk had nearly no protein denaturation after 10 min of processing (X = 0.95 and 0.96 for experimental and simulated, respectively). In the case of egg white, it was slightly small, but it remained 0.87 and 0.84 for experimental and simulated, respectively, and it were 0.89 and 0.85 for whole egg.

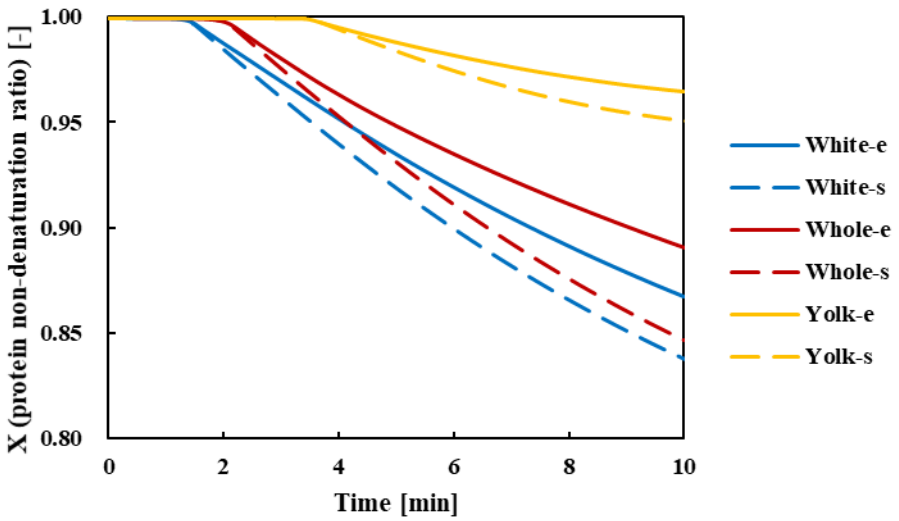

Fig 4-10 Protein non-denaturation ratio (X) of liquid egg samples during OH (20 kHz and 50 V) plus thermal keeping stage (experimental and simulated approaches 1 and 2). e: experimental result, s: simulated result.

4.3.2 Temperature, pasteurization value, and *X* evaluation of egg samples of Model 2

(1) temperature evaluation of egg samples during processing

The temperature distributions at the end of approaches 3 and 4 (**Fig. 4-11**) were more uniform than those without external heating. The temperature distribution results showed nearly no temperature difference at several internal cross-sections of the liquid egg samples, confirming temperature homogeneity after a total process time of 10 min. The temperature distribution results of simulated approach 4 were the best in terms of temperature uniformity. The temperature difference between the hot and cold spots of liquid egg samples using approach 4 was 1.7, 1.8, and 1.9 °C for egg white, whole egg, and egg yolk, respectively. Because liquid egg whites registered the shortest OH time (89 s) to achieve the target temperature, it took the longest time to reduce the temperature difference via external heating. Meanwhile, under the approach 4 the OH times of whole egg and egg yolk to achieve target temperature were 129 s and 212 s, respectively, slightly shorter than the time observed with approach 1 because of the influence of the external heating system. The prolonged process times of whole eggs and egg yolks compared to egg whites limits the available external heating time, which is necessary to reduce the temperature difference between the hot and cold spots.

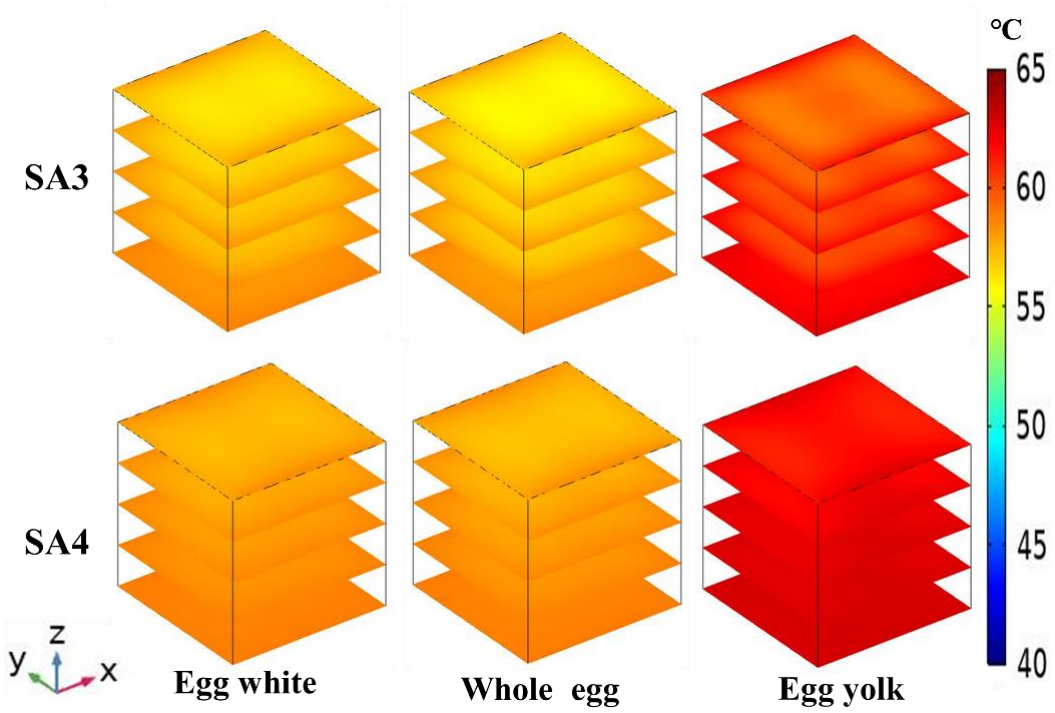

Fig. 4-11 Temperature distribution in the horizontal cross sections of liquid egg samples during the OH process (20 kHz and 50 V) (at the end of OH treatment and thermal keep processing; simulated approach 3 – SA3, at the end of OH treatment plus external heating [external heating started after OH treatment]; and simulated approach 4 – SA4, at the end of OH treatment plus concurrent external heating [for simulated approaches 3, and 4, the total processing time was 10 min]). Egg samples were connected to the electrodes in the X-axis direction.

(2) Pasteurization effect evaluation

For simulated approach 3 (**Fig. 4-12**), it was confirmed that the pasteurization standard was completely achieved for the entire sample after 523 s and 904 s for egg white and egg yolk, respectively. However, for whole egg samples, the *P*-value standard was not completely reached even after 20 min, with lower *P*-values at the top surface (a part that was not covered by the external heating system). Moreover, the egg whites and egg yolks overheated, especially at the edges and bottom. On the other hand, after 5 min of heating (OH only), lower *P*-values were observed with approach 3 than with approach 2 because of the differences in the thermophysical properties of the containers.

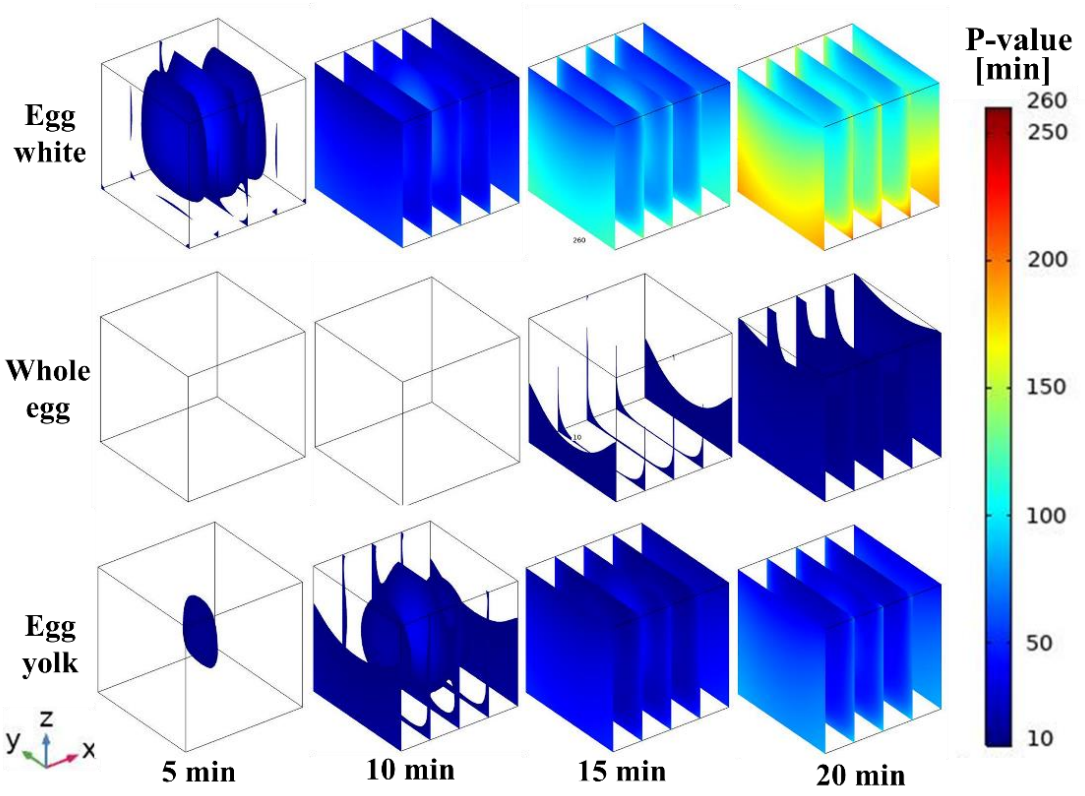

Fig. 4-12 Simulated P-value distributions (for P-values ⩾ 10) at several vertical cross sections of liquid egg samples and time intervals during the OH treatment process at 20 kHz and 50 V, under simulated approaches 3. Liquid egg samples were connected to the electrodes in the X-axis direction.

For simulated approach 4 (**Fig. 4-13**), the previously reported problems in achieving the standard *P*-values were not observed. Shorter heating times (422, 603, and 1083 s for egg white, egg yolk, and whole egg, respectively) were confirmed. However, the applied heating time should be controlled to avoid overheating because of the unnecessary elongation of the processing time. A better uniformity distribution of temperature and *P*-values was evident after the inclusion of external heating at all surfaces, except the top surface. These results have the potential to help in the design of OH processes used in combination with novel external heating systems.

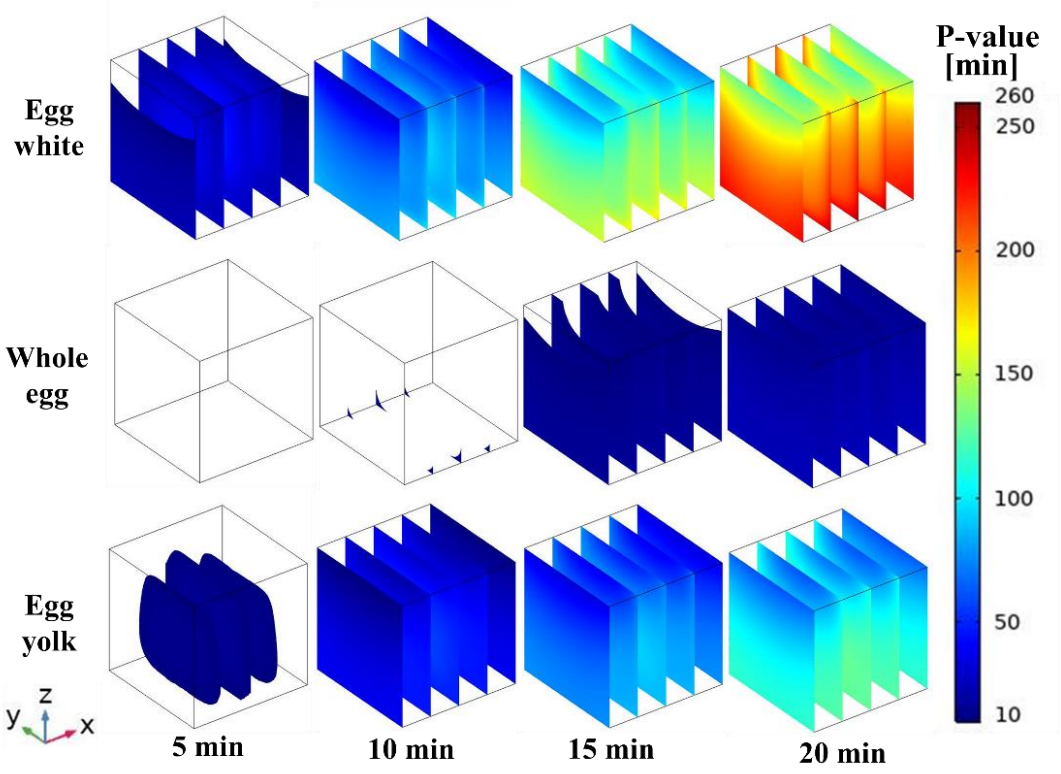

Fig. 4-13 Simulated P-value distributions (for P-values ⩾ 10) at several vertical cross sections of liquid egg samples and time intervals during the OH treatment process at 20 kHz and 50 V, under simulated approaches 4. Liquid egg samples were connected to the electrodes in the X-axis direction.

(3) Protein denaturation evaluation

The protein denaturation evaluation standard of liquid egg samples is same as Model 1 in section 4.3.1.

As shown in **Fig. 4-14**, the degree of protein denaturation of liquid egg samples was evaluated using the protein non-denaturation ratio (X) under simulated approaches 3, and 4. From the results, it can be concluded that egg yolk had nearly no protein denaturation after 10 min of processing. In the case of egg white, it was slightly small, but it remained above 0.8, and it could keep going higher (X = 0.88) as the egg white samples achieve the pasteurization standard at 422 s. It can be considered that the protein denaturation of egg samples was not severe, and the quality of the samples were almost retained even after processing. The degree of denaturation of the liquid whole egg was evaluated based on the egg white portion because this protein was more easily denatured than the yolk portion. Since the whole egg samples required a longer heating time (1083 s) to achieve the pasteurization standard, their X value was smaller (X = 0.69) than the white and yolk samples.

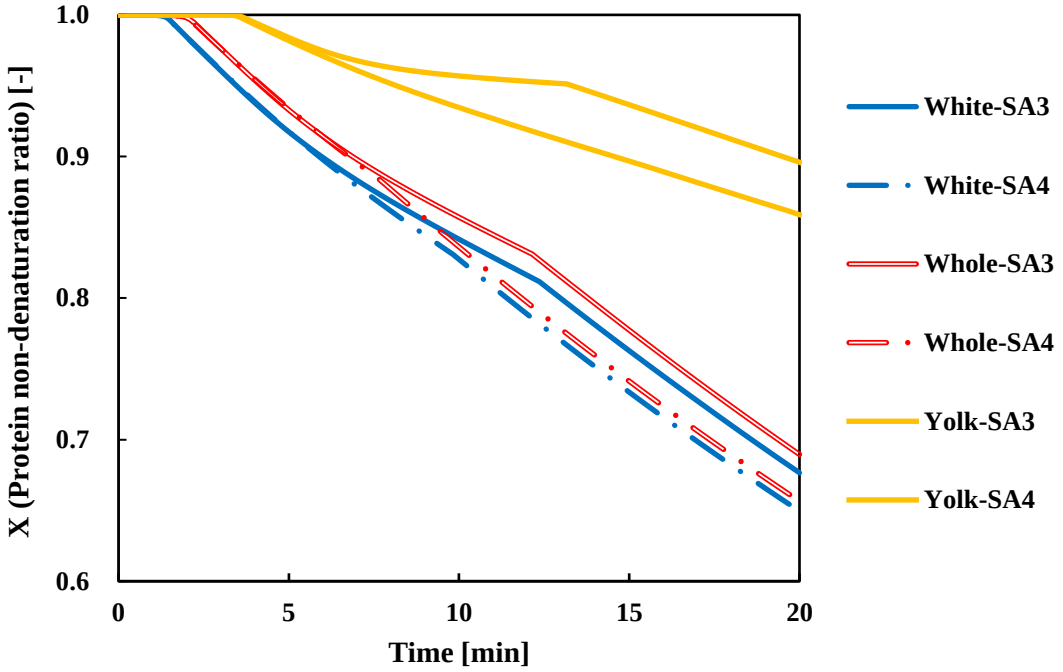

Fig. 4-14 Protein non-denaturation ratios (X) of liquid egg samples (calculated depending on the temperature of the hot spot) during processing. SA3: simulated approach 3, SA4: simulated approach 4.

(4) Compliance with pasteurization standards

In **Fig. 4-15**, with the inclusion of the concurrent external heating approach (simulated approach 4), it was confirmed that the temperature difference between the hot and cold spots was much smaller than that reported in **Fig. 4-8 and 4-11** (using the experimental approaches 1 or 2). For comparison, the process was extended until the egg sample which took the longest processing time (whole egg) reached the desired pasteurization standard. The time required to achieve the pasteurization standard was 422, 603, and 1083 s for egg white, egg yolk, and whole egg, respectively. At these times, the protein non-denaturation ratios for egg white, egg yolk, and whole egg were 0.88, 0.93, and 0.69, respectively.

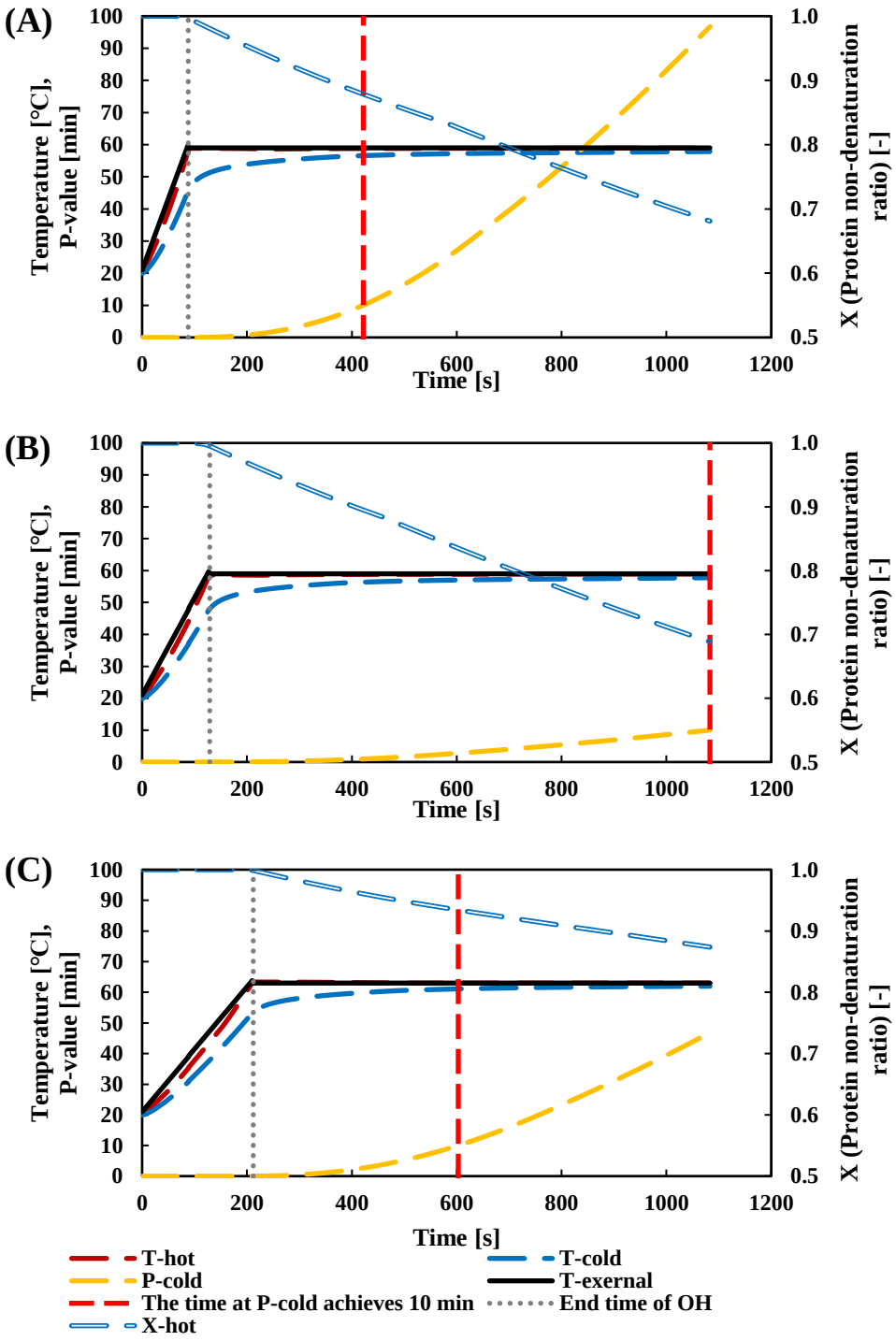

Fig. 4-15 Simulated profiles of temperatures, *P*-values, and protein non-denaturation ratios (*X*) of liquid egg samples during OH processing (20 kHz and 50 V): egg white (A), whole egg (B), and egg yolk (C) under simulation approach 4 (OH plus concurrent external heating). The black line is the external heating system (T-external) temperature, the grey dotted line is the end of OH, and the red dotted line is the time where *P*-cold = 10 min.

In this study, although the non-thermal effects during microbial inactivation via OH have not been determined, these newly developed approaches showed a good pasteurization effect. It has been reported that OH has larger decimal reduction times, shorter heating times, and smaller temperature gradients than conventional heating methods under most conditions, even in the absence of non-thermal effects (Müller et al., 2020).

4.4 Conclusion

The temperature distribution of food materials such as liquid eggs during OH could be analyzed and predicted by computer simulation accurately. In this study, we confirmed that some non-uniformities in temperature distribution during OH pasteurization occurred, although it is well known as a volumetric heating method which offers better temperature uniformity than traditional methods. And it was found that OH combined with a concurrent external heating approach was successful in reducing non-uniformities in temperature, which could accomplish the pasteurization standards for liquid egg samples while avoiding excessive thermal protein denaturation caused by local overheating. Using this approach, liquid egg white, whole egg, and egg yolk could achieve the pasteurization standard after 422, 1083, and 603 s, respectively, while keeping X values at 0.88, 0.69, and 0.93, respectively.

Although OH has been confirmed as an efficient pasteurization method for delicate samples such as liquid eggs, the processing conditions should be optimized, especially when they are synergistically used with external heating methods, as was explored in this study. Experimental validation of the developed simulation approaches is required for further studies.

4.5 References

Cappato, L. P., Ferreira, M. V., Guimaraes, J. T., Portela, J. B., Costa, A. L., Freitas, M. Q., et al. (2017). Ohmic heating in dairy processing: Relevant aspects for safety and quality. *Trends in Food Science & Technology*, 62, 104–112.

Coimbra, J. S., Gabas, A. L., Minim, L. A., Rojas, E. E. G., Telis, V. R., & Telis-Romero, J. (2006). Density, heat capacity and thermal conductivity of liquid egg products. *Journal of Food Engineering*, 74(2), 186–190.

Engchuan, W., Jittanit, W., & Garnjanagoonchorn, W. (2014). The ohmic heating of meat ball: Modeling and quality determination. *Innovative Food Science & Emerging Technologies, 23*, 121-130.

Garibaldi, J. A., Straka, R. P., & Ijichi, K. (1969). Heat resistance of Salmonella in various egg products. *Applied Microbiology*, 17(4), 491–496.

Guo, W., Llave, Y., Jin, Y., Fukuoka, M., & Sakai, N. (2017). Mathematical modeling of ohmic heating of two-component foods with non-uniform electric properties at high frequencies. *Innovative Food Science and Emerging Technologies*, 39, 63–78.

Jin, Y., Jiang, C., Jiao, Y., Llave, Y., Fukuoka, M., & Sakai, N. (2020). Analysis of ohmic heating of yellowtail (Seriola quinqueradiata) fillets at high frequencies by 3D simulation—Effect of ohmic heating system (batch and pseudo-continuous), sample shape, and size. *Innovative Food Science & Emerging Technologies*, 66, 102482.

Jun, S., & Sastry, S. (2007). Reusable pouch development for long term space missions: A 3D ohmic model for verification of sterilization efficacy. *Journal of Food Engineering, 80*(4), 1199-1205.

Knirsch, M. C., Dos Santos, C. A., Vicente, A., & Penna, T. C. V. (2010). Ohmic heating–a review. *Trends in Food Science & Technology*, 21(9), 436–441.

Llave, Y., Fukuda, S., Fukuoka, M., Shibata-Ishiwatari, N., & Sakai, N. (2018b). Analysis of color changes in chicken egg yolks and whites based on degree of thermal protein denaturation during ohmic heating and water bath treatment. *Journal of Food Engineering*, 222, 151–161.

Marra, F., Zell, M., Lyng, J. G., Morgan, D. J., & Cronin, D. A. (2009). Analysis of heat transfer during ohmic processing of a solid food. *Journal of Food Engineering*, 91(1), 56–63.

Mercali, G. D., Schwartz, S., Marczak, L. D. F., Tessaro, I. C., & Sastry, S. (2014). Ascorbic acid degradation and color changes in acerola pulp during ohmic heating: Effect of electric field frequency. *Journal of Food Engineering*, 123, 1–7.

Müller, W. A., Marczak, L. D. F., & Sarkis, J. R. (2020). Microbial inactivation by ohmic heating: Literature review and influence of different process variables. *Trends in Food Science & Technology*, 99, 650–659.

Seyhun, N., Ramaswamy, H. S., Zhu, S., Sumnu, G., & Sahin, S. (2013). Ohmic tempering of frozen potato puree. *Food and Bioprocess Technology*, 6(11), 3200–3205.

Tumpanuvatr, T., & Jittanit, W. (2012). The temperature prediction of some botanical beverages, concentrated juices and purees of orange and pineapple during ohmic heating. *Journal of Food Engineering, 113*(2), 226-233.

COMSOL (2017). How to inspect your mesh in COMSOL Multiphysics® - COMSOL Blog. https://www.comsol.com/blogs/how-to-inspect-your-mesh-in-comsol-multiphysics (accessed July 29, 2021).

COMSOL (2020a). AC/DC module user's guide (5.6 version), 218–222. https://doc.comsol.com/5.6/doc/com.comsol.help.acdc/ACDCModuleUsersGuide.pdf Accessed May 28, 2021.

COMSOL (2020b). Heat transfer module user's guide (5.6 version), 105–318. https://doc.comsol.com/5.6/doc/com.comsol.help.heat/HeatTransferModuleUsersGuide.pdf Accessed May 28, 2021.

COMSOL (2021a). Natural Convection Cooling of a Vacuum Flask (Application ID: 1448). Retrieved from https://www.comsol.jp/model/natural-convection-cooling-of-a-vacuum-flask-1448. Accessed May 28, 2021.

MEXT, Ministry of Education, Culture, Sports, Science and Technology-Japan (2015). Standard tables of food composition in Japan – 2015 – (7th revised version). https://www.mext.go.jp/component/a_menu/science/detail/__icsFiles/afieldfile/2017/02/16/1365343_1-0212r9.pdf. Accessed May 28, 2021.

MHLW, Ministry of Health, Labour and Welfare (1959). Standards for each food, bird egg. https://www.mhlw.go.jp/file/06-Seisakujouhou-11130500-Shokuhinanzenbu/0000094499.pdf. Accessed May 28, 2021.

Chapter 5 – Conclusions

This study focused on the ohmic heating of liquid eggs for pasteurization. High OH frequency (20 kHz) at 50 V was used to provide electricity power for the whole system. The electrical conductivity of sample as a critical factor in OH research was calculated from electrical properties measured by an amperemeter and a voltmeter, and temperature as well as frequency dependency of electrical conductivity was examined. Temperature histories at different locations of liquid eggs during heating were measured and compared with simulated results, which proved the credibility of simulation models. Pasteurization values of liquid eggs were calculated depending on the temperature profiles for pasteurization effect evaluation. Thermal protein non-denaturation ratios of liquid eggs were also calculated depending on the temperature profiles and combined with color changes for quality evaluation. The pasteurization conditions were optimized by combining OH with external heating approach using computer simulation, which could accomplish the pasteurization standards for liquid egg samples while avoiding excessive thermal protein denaturation caused by local overheating.

In chapter 1, the backgrounding (such as advantages against traditional thermal methods, novel pasteurization methods developments of liquid eggs, important parameters in OH) of ohmic heating technology has been introduced. Objectives of this study were stated, and structure of this dissertation was displayed.

In chapter 2, it was found out that the electrical conductivities (EC) of the liquid egg samples showed a good linear relationship with temperature, and these EC values increased linearly with increasing temperature in the evaluated temperature range (20 °C–63.3 °C). The EC values of egg yolk and white were the smallest and the largest, respectively, while the EC values for whole eggs were between them during OH..

In chapter 3, the temperature non-uniformity at of liquid egg samples occurred during OH pasteurization, which had a direct impact into accomplish pasteurization standards in delicate samples such as liquid eggs. Although it can be observed that the center of egg white and yolk achieved the pasteurization standard (*P*-value above 10 min) after a short processing time, the P-values at the top corner remained at approximately 0 because the temperature it reached was not high enough. In the case of whole eggs, the pasteurization standard was not reached even at the center. The liquid egg samples kept high quality (*X* values kept high and the color had nearly no change) after 10 min processing (including OH and thermal

keep approaches), but considering that the pasteurization effect had not fully achieved the standards, the heating conditions needed to be further considered and optimized.

In chapter 4, finite element method was used to do the simulation using COMSOL Multiphysics 5.6 software, the temperature distribution of food materials such as liquid eggs during OH were analyzed and predicted by computer simulation accurately. In this study, we confirmed that some non-uniformities in temperature distribution during OH pasteurization occurred. And it was found that OH combined with a concurrent external heating approach was successful in reducing non-uniformities in temperature, which could accomplish the pasteurization standards for liquid egg samples while avoiding excessive thermal protein denaturation caused by local overheating.

Although OH has been confirmed as an efficient pasteurization method for delicate samples such as liquid eggs, the processing conditions should be optimized, especially when they are synergistically used with external heating methods, as was explored in this study. Experimental validation of the developed simulation approaches is required for further studies. These research works have the potential to improve the state of the art of pasteurization processing of liquid eggs and other delicate food products that can be benefited by the pasteurization technical developments through the conduction of this proposed research work, and the application of these developments would lead to more efficient and energy saving processing of high quality and value-added food products, which is benefit to reducing food and energy waste, and contributing on the Sustainable Development Goals.

Nomenclature

a^* Egg surface color on red/green axis of $L^*a^*b^*$ color spaces (-)

A Area (m^2)

b^* Egg surface color on blue/yellow axis of $L^*a^*b^*$ color spaces (-)

B' Egg surface color on blueness axis of *RGB* color spaces (-)

C Concentration of non-denatured protein ($mol \cdot g^{-1}$)

C_P Specific heat capacity ($J \cdot kg^{-1} \cdot K^{-1}$)

D Electric displacement ($C \cdot m^{-1}$)

E Electric field (V)

E_a Activation energy ($kJ \cdot mol^{-1}$)

G' Egg surface color on greenness axis of *RGB* color spaces (-)

h Heat transfer coefficient ($W \cdot m^{-2} \cdot K^{-1}$)

I Current (A)

$I_{j,v}$ Volumetric source of current ($A \cdot m^{-3}$)

J Current density ($A \cdot m^{-3}$)

Je Externally generated current density ($A \cdot m^{-2}$)

k Thermal conductivity ($W \cdot m^{-1} \cdot K^{-1}$)

k_t Reaction rate constant (min^{-1})

L Distance (m)

L^* Egg surface color lightness of $L^*a^*b^*$ color spaces (-)

P Thermal pasteurization value (min)

q Conductive heat flux ($W \cdot m^{-2}$)

Q Heat source ($W \cdot m^{-3}$)

R Electrical resistance (Ω)

R' Egg surface color on redness axis of *RGB* color spaces (-)

R_t Molar gas constant ($J \cdot K^{-1} \cdot mol^{-1}$)

Ra_L Rayleigh number (-)

t Heating time (s or min)

t_0 Total heating time of liquid egg sample from beginning to target temperature (s)

T Temperature (°C or K)

T_{amb} The ambient temperature during simulation (℃)

T_{ext} Temperature of external heating system during processing (℃)

T_{ref} Thermal pasteurization standard temperature of egg sample (℃)

T_t Thermal protein denaturation beginning temperature of egg samples (℃)

T_1 Temperature of liquid egg samples at beginning (℃)

T_2 Temperature of external heating system at beginning (℃)

u Air velocity field ($m \cdot s^{-1}$)

U Voltage (V)

V Electric potential (V)

W_w Water content in mass fraction of egg materials (-)

X Non-denaturation ratio (-)

X' Egg surface color on redness axis of *XYZ* color spaces (-)

Y' Egg surface color on greenness axis of *XYZ* color spaces (-)

Z Pre-exponential factor of Arrhenius equation (min^{-1})

Z' Egg surface color on blueness axis of *XYZ* color spaces (-)

Z_e Electrical impedance (Ω)

Z_t Slope of thermal destruction time curves for *S. typhimurium* (℃)

ΔE^* Total color difference (-)

ΔC^* Difference in chroma (color saturation) (-)

Greek symbol

σ Electrical conductivity ($S \cdot m^{-1}$)

ρ Density ($kg \cdot m^{-3}$)

μ Dynamic viscosity (Pa·s)

Subscripts

a *air*

c cold spot

e experimental

h hot spot

i ovalbumin for egg white and whole egg, and low-density lipoproteins for egg yolk

s simulated

Acknowledgement

I would like to express my sincere appreciation firstly to Professor Noboru Sakai, who helped me a lot during my Junior year studies at Tokyo University of Marine Science and Technology as an international exchange student, and it was at that time I began to get in touch with food thermal processing and became interested in it. Secondly, my gratitude shall be paid to Professor Mika Fukuoka, who has always been gentle and supportive. She always points out the direction for me when I encounter difficulties in my study and help me solve problems, so that I can be full of hope and confidence to continue my study. And another person I would like to acknowledge very much is Professor Yvan Llave. He inspired me with his profound knowledge in the field of thermal processing and the enthusiastic attitude towards study. And he gave me kind support at any time.

I would like to express my gratitude, for Professor Watanabe and Professor Hagiwara to take time in their busy schedule to review this paper of mine.

Also, I would like to express my sincere appreciation to all the members Food Thermal Processing Laboratory, Tokyo University of Marine Science and Technology who have generously offered help to me all the time.

Gratitude to all the friends of mine, who helped me all the time, and make my life and study better.

Gratitude to Tokyo University of Marine Science and Technology for the convenience of my study and life.

I would like to appreciate Zhang Lie, my senior, friend, comrade, and beloved, for the understanding, companionship, and support from her, all the time. And thanks to Food Thermal Processing Laboratory for bringing us together.

Gratitude to my parents, who gave me support and encouragement all the time.

Last but not the least, I would like to express my sincere gratitude to my motherland, the People's Republic of China under the leadership of the Communist Party of China. No matter when and where, she is my most strong backing. In the future, I will continue to work hard to shoulder the obligations to my family, society and country, remain true to my original aspiration and keep my mission firmly in mind.